

RESEARCH ARTICLE

PCNA antagonizes cohesin-dependent roles in genomic stability

Caitlin M. Zuilkoski [‡], Robert V. Skibbens ^{*}

Department of Biological Sciences, Lehigh University, Bethlehem, Pennsylvania, United States of America

[‡] Current address: Department of Biology, Indiana University, Bloomington, Indiana, United States of America^{*} rvs3@lehigh.edu OPEN ACCESS**Citation:** Zuilkoski CM, Skibbens RV (2020) PCNA antagonizes cohesin-dependent roles in genomic stability. PLoS ONE 15(10): e0235103. <https://doi.org/10.1371/journal.pone.0235103>**Editor:** Michael Polymenis, Texas A&M University College Station, UNITED STATES**Received:** June 7, 2020**Accepted:** October 4, 2020**Published:** October 19, 2020**Copyright:** © 2020 Zuilkoski, Skibbens. This is an open access article distributed under the terms of the [Creative Commons Attribution License](https://creativecommons.org/licenses/by/4.0/), which permits unrestricted use, distribution, and reproduction in any medium, provided the original author and source are credited.**Data Availability Statement:** All original images (gels, blots, etc.), and underlying data and findings are available at FigShare under the following DOI: [10.6084/m9.figshare.12908282](https://doi.org/10.6084/m9.figshare.12908282).**Funding:** This study was funded through an award from the National Institutes of Health [R15GM110631] to R.V.S. and a Nemes Fellowship Research Award to CMZ. The funders had no role in study design, data collection and analysis, decision to publish, or preparation of the manuscript.**Competing interests:** The authors have declared that no competing interests exist.

Abstract

PCNA sliding clamp binds factors through which histone deposition, chromatin remodeling, and DNA repair are coupled to DNA replication. PCNA also directly binds Eco1/Ctf7 acetyltransferase, which in turn activates cohesins and establishes cohesion between nascent sister chromatids. While increased recruitment thus explains the mechanism through which elevated levels of chromatin-bound PCNA rescue *eco1* mutant cell growth, the mechanism through which PCNA instead worsens cohesin mutant cell growth remains unknown. Possibilities include that elevated levels of long-lived chromatin-bound PCNA reduce either cohesin deposition onto DNA or cohesin acetylation. Instead, our results reveal that PCNA increases the levels of both chromatin-bound cohesin and cohesin acetylation. Beyond sister chromatid cohesion, PCNA also plays a critical role in genomic stability such that high levels of chromatin-bound PCNA elevate genotoxic sensitivities and recombination rates. At a relatively modest increase of chromatin-bound PCNA, however, fork stability and progression appear normal in wildtype cells. Our results reveal that even a moderate increase of PCNA indeed sensitizes cohesin mutant cells to DNA damaging agents and in a process that involves the DNA damage response kinase Mec1(ATR), but not Tel1(ATM). These and other findings suggest that PCNA mis-regulation results in genome instabilities that normally are resolved by cohesin. Elevating levels of chromatin-bound PCNA may thus help target cohesinopathic cells linked that are linked to cancer.

Introduction

During S phase, the cellular genome duplicates and each sister chromatid becomes tethered together to ensure proper inheritance of the genome during mitosis. Sister chromatid tethering is maintained by cohesin, a complex comprised of Smc1, Smc3, and Mcd1/Sccl/RAD21 along with auxiliary subunits Pds5, Sccl/Irr1, Rad61/WAPL and, in vertebrate cells, Sororin [1–7]. Cohesin deposition onto DNA requires the cohesin loader, comprised of Sccl and Sccl4, which functions through a large part of the cell cycle but is essential during S phase for cohesins to participate in sister chromatid tethering [8, 9]. Deposition onto chromatin, however, is not sufficient for cohesion. Eco1/Ctf7 (herein Eco1) is an acetyltransferase that converts

chromatin-bound cohesins, through acetylation of Smc3 cohesin subunit, to a tethering competent state [3, 10–13]. Early studies coupled this process of cohesion establishment to the DNA replication factor PCNA [10]. PCNA directly binds and recruits Eco1 to the DNA replication fork [14–16], suggesting that establishment is coordinated with numerous processes (histone deposition, chromatin remodeling, DNA repair and translesion synthesis) directed by PCNA and regulated through PCNA post-translational modifications [17–20]. Elevated recruitment to the DNA replication fork thus provides a plausible explanation for PCNA-dependent suppression of *eco1* mutant cell growth defects [10, 15]. In support of this model, genetic fusing of *ECO1* and *POL30* (PCNA) restores cohesion defects otherwise present in *eco1* PIP box mutants [21]. The repertoire of DNA replication factors (Chl1, Ctf4, Ctf18, MCM2-7, for example) implicated in cohesion establishment regulation has grown substantially [15, 22–36], highlighting the fundamental and highly conserved nature through which cohesion establishment is obligatorily coordinated with DNA replication.

Further complicating the relationship between PCNA, Eco1 and cohesins are the additional roles played beyond sister chromatid tethering [1, 5, 10, 21, 37–48]. For instance, cohesin functions in both DNA replication restart during S phase and high fidelity DNA repair after S phase [49–51]. Cohesin is recruited to stalled DNA replication forks during S phase, as well as to rDNA and telomeric regions that experience prescribed pauses during replication [52–54]. Cohesin is similarly recruited to sites of DNA damage to promote high fidelity repair by ensuring proximity to the undamaged sister template [50, 55, 56]. Intriguingly, once recruited to stalled replication forks and sites of DNA damage, cohesin must ultimately dissociate from DNA to promote replication fork restart [57]. Thus, cohesin and PCNA appear to play highly coordinated roles in DNA metabolism.

PCNA impact on cohesin complexes, however, is quite complex. Deletion of the PCNA-dissociation factor *ELG1* (*elg1Δ*), or simply overexpression of PCNA (PCNA^{OE}), result in long-lived retention and increased levels of chromatin-bound PCNA which in turn rescues *eco1* and *pds5* mutant cell cohesion defects and viability [10, 15, 32–34, 58–63]. Conversely, *elg1Δ* and PCNA^{OE} each exacerbate the growth defects exhibited by cohesin (*mcd1*, *smc1* and *smc3*) mutant cells [15, 32, 33, 35]. The mechanism through which elevated levels of chromatin-bound PCNA antagonize cohesin mutant cell growth remains unknown, highlighting a critical deficit in current descriptions of cohesin regulation. In this current study, we confirm the adverse impact that PCNA^{OE} exerts on cohesin mutant strains, even while having no overt adverse effect in wildtype cells. We then test multiple mechanisms through which the long-lived retention, and increased levels, of chromatin-bound PCNA exacerbates cohesin mutant cells: models that include competition for DNA access, changes in cohesin acetylation states, and increased sensitivity to genotoxic agents.

Materials and methods

Yeast strains and bacterial plasmids

All reagents, yeast strains, and bacterial plasmids are listed in S1–S3 Tables, respectively. All yeast strains used in this study were performed in a W303 background strain unless otherwise noted (S2 Table). V5 tagged Smc3 strains were created using EU3430-9A, generously given by Drs. Vincent Guacci and Douglas Koshland. Primers used to amplify the SMC3:V5:HIS region, primers are (forward primer) 5'-TTAACGCGGTTGATTTCTACTTTCCAAAAGGTTTCTGAAAA-3' and (reverse primer) 5'-TAGCTCTGATTCTGACTCTAACTCCAGTTCGGACTCCGTATCGGATTCCAGTTCAGATTC-3'. The resulting PCR product was transformed into a wildtype W303 background strain (YCZ044) to produce YCZ249. YCZ249 was mated with YCZ262 and a genetic cross was used to obtain YCZ280. YCZ280 was mated with YBS2012 to

obtain YCZ407, YCZ408, YCZ425, and YCZ428 (see [S2 Table](#)). A CEN vector plasmid or 2μ *POL30* plasmid were transformed into YCZ147 and YCZ144 to obtain the resulting yeast strains: YCZ477, YCZ465, YCZ474, and YCZ225. YCZ559, YCZ561, YCZ563, and YCZ565 were created by transforming either a CEN vector plasmid or 2μ *POL30* plasmid into K5824 and K6013, respectively, generously given by Dr. Vincent Guacci. A CEN vector plasmid or 2μ *POL30* plasmid were transformed into YMM433 and YMM435 to obtain the resulting yeast strains (YCZ530, YCZ532, YCZ534, YCZ536). A CEN vector plasmid or 2μ *POL30* plasmid were transformed into YDM884 and DLY285 to obtain the resulting yeast strains (YCZ567 through YCZ578). A pGADT7 vector plasmid or a 2μ *ADH AD:HA:POL30* plasmid was transformed into yeast strains K699, K5824, and K6013 to generate resulting yeast strains (YCZ662 through YCZ673). 2μ *POL30* plasmid was transformed into yeast strains K5824 and K6013 to generate resulting yeast strains (YCZ559, YCZ561, YCZ563, YCZ565). Primers (forward primer) 5'-AGAGAAGGTTTTCCAATGAAAAGGCACGTGTCTTTATCTGATATATTGACAGGAAATAAGCGGATCCCCGGGTTAATTAA-3' and (reverse primer) 5'-ATTTCCCCGCACTACCATGCTATATTTATTATACATACGTGTTCTGTAAACGATGCACGCGAATTCGAGCTCGTTTAAAC-3' were used to generate strains harboring *ELG1::KAN* as previously described [64]. The resulting PCR product was transformed into K5824 to obtain the yeast strains YCZ706 and YCZ707. YCZ143 was mated to K6013 to obtain YCZ702 and a genetic cross was used to obtain YCZ728 and YCZ729. CZ421 was mated to CZ778, generously given by Dr. Gregory Lang, to obtain CZ799 and a genetic cross was used to determine the genetic interaction between *msh3Δ*, *elg1Δ*, and *mcd1-1* alleles. Strains and plasmids are available upon request.

Dilution plating

Cells were grown at 23° overnight in either YPD or selection media, normalized by OD600, and then plated in 10-fold serial dilutions at the indicated temperatures on YPD medium or selective medium. Cells grown on YPD medium or selective medium supplemented with methyl methanesulfonate (Sigma) or hydroxyurea (Sigma) were treated in a similar manner.

Smc3 chromatin binding assay

Log phase yeast strains were grown to 0.6 OD600 and synchronized in G1 by exposing cells to fresh media supplemented with alpha factor at the permissive temperature of 23°C for three hours. The resulting G1 synchronized cells were washed, cultures split in half and maintained for three hours at 34°C or 37°C for 3 hours. Nocodazole arrested cells were harvested to assess Smc3 chromatin binding levels, based on modifications of previously described protocols [65]. Cell cultures were normalized to OD600 between 0.3–0.6, pelleted and washed with 1.2 M Sorbitol. Cells were resuspended in CB1 buffer (50 mM Sodium citrate, 1.2 M Sorbitol, 40 mM EDTA, pH 7.4) and spheroblasted. Spheroblasted cells were washed, resuspended in 1.2 M Sorbitol, and frozen in liquid nitrogen. Cells were thawed on ice and supplemented with Lysis buffer (500 mM Lithium Acetate, 20 mM MgSO₄, 200 mM HEPES, pH 7.9), protease inhibitor cocktail (AEBSF, 1,10-Phenanthroline, Pepstatin A, E-64) (Sigma), and TritonX-100. Lysates were centrifuged at 12,000g for 15 minutes and soluble and containing chromatin bound fractions collected and denatured using 2X Laemmli buffer. Whole cell extracts, supernatant, and pellet were resolved by SDS-PAGE and analyzed by Western blot using anti-V5 (1:40,000) (Invitrogen) with goat anti-mouse HRP (1:40,000) (Bio-Rad), anti-PGK (1:20,000) (Novex) with goat anti-mouse HRP (1:40,000) (Bio-Rad), or anti-H2B (1:80,000) (Abcam) with goat anti-rabbit HRP (1:40,000) (Bio-Rad) and ECL prime (GE Healthcare) for visualization.

Smc3 acetylation assay

Log phase yeast strains were grown to 0.6 OD600 and synchronized in G1 by exposing cells to fresh media supplemented with alpha factor at the permissive temperature of 23°C for three hours. The resulting G1 synchronized cells were washed, cultures split in half and maintained for three hours at 34°C or 37°C. Nocodazole arrested cells were harvested to assess Smc3 acetylation, with additional modifications as previously described [65]. Cell cultures were normalized to an OD600 between 0.3–0.6. Cells were washed in sterile water, then resuspended in sterile water prior to freezing at -80°C. Frozen pellets were extracted by the addition of IPH50 buffer (50mM Tris pH 7.8, 150mM NaCl, 5mM EDTA, 0.5% IGEPAL 630 (Sigma), 10mM Sodium Butyrate, 1mM DTT) and glass beads prior to bead beating (BioSpec). Cell lysates were supplemented with IPH50 buffer and protease inhibitor cocktail (AEBSF, 1,10-Phenanthroline, Pepstatin A, E-64) (Sigma), centrifuged at 15,000rpm for 20 minutes, and the pellet washed with sterile water before centrifugation at 15,000rpm for 10 minutes. The resulting chromatin fraction was supplemented with SBIIA buffer (0.5M Tris pH 9.4, 6% Sodium Dodecyl Sulfate before a 10-minute incubation at 50°C. SBII buffer (50% glycerol supplemented with bromophenol blue) and 1M DTT buffer was added to the cell lysates followed by a 5-minute incubation at 65°C. Whole cell protein samples were resolved by SDS-PAGE electrophoresis and analyzed by Western blot using anti-V5 (1:40,000) (Invitrogen) with goat anti-mouse HRP (1:40,000), anti-PGK (1:20,000) (Novex) with goat anti-mouse HRP (1:40,000) (Bio-Rad) or by anti-Smc3 K112/K113 Acetylation (1:1,000, gift from Dr. Katsuhiko Shirahige) in combination with goat anti-mouse HRP (1:10,000) (Bio-Rad) and ECL prime (GE Healthcare) for visualization.

PCNA chromatin binding assay

Log phase yeast strains were normalized to OD600 between 0.3–0.6, pelleted and washed with 1.2 M Sorbitol. Cells were resuspended in CB1 buffer (50 mM Sodium citrate, 1.2 M Sorbitol, 40 mM EDTA, pH 7.4) and spheroblashed. Spheroblashed cells were washed, resuspended in 1.2 M Sorbitol, and frozen in liquid nitrogen. Cells were thawed on ice and supplemented with Lysis buffer (500 mM Lithium Acetate, 20 mM MgSO₄, 200 mM HEPES, pH 7.9), protease inhibitor cocktail (AEBSF, 1,10-Phenanthroline, Pepstatin A, E-64) (Sigma), and TritonX-100. Lysates were centrifuged at 12,000g for 15 minutes and soluble and containing chromatin bound fractions collected and denatured using 2X Laemelli buffer. Whole cell extracts, supernatant, and pellet were resolved by SDS-PAGE and analyzed by Western blot using anti-PCNA (1:1,000) (Abcam) with rabbit anti-mouse HRP (1:40,000) (Bio-Rad), anti-PGK (1:20,000) (Novex) with goat anti-mouse HRP (1:40,000) (Bio-Rad), or anti-H2B (1:80,000) (Abcam) with goat anti-rabbit HRP (1:40,000) (Bio-Rad) and ECL prime (GE Healthcare) for visualization.

Rad53 phosphorylation assay

Log phase yeast strains were grown to 0.6 OD600 and synchronized in G1 by exposing cells to fresh media supplemented with alpha factor at the permissive temperature of 23°C for three hours. The resulting G1 synchronized cells were washed, and half of the wildtype cell culture was exposed to 0.05% MMS to induce Rad53 phosphorylation. Cultures were then maintained for three hours at 37°C. Nocodazole arrested cells were harvested to assess Rad53 phosphorylation, with additional modifications as previously described [65]. Cell cultures were normalized to an OD600 between 0.3–0.6. Cells were washed in sterile water, then resuspended in sterile water prior to freezing at -80°C. Frozen pellets were extracted by the addition of Trichloroacetic acid (TCA) and glass beads prior to bead beating (BioSpec). Cell lysates were supplemented

with TCA, centrifuged at 15,000rpm for 20 minutes, and the pellet washed with sterile water before centrifugation at 15,000rpm for 10 minutes. The resulting chromatin fraction was supplemented with SBIIA buffer (0.5M Tris pH 9.4, 6% Sodium Dodecyl Sulfate before a 10-minute incubation at 50°C. SBII buffer (50% glycerol supplemented with bromophenol blue) and 1M DTT buffer was added to the cell lysates followed by a 5-minute incubation at 65°C. Whole cell protein samples were resolved by SDS-PAGE electrophoresis and analyzed by Western blot using anti-Rad53 (1:5,000) (Invitrogen) with goat anti-mouse HRP (1:30,000) or by anti-PGK (1:20,000) (Novex) with goat anti-mouse HRP (1:40,000) (Bio-Rad) and ECL prime (GE Healthcare) for visualization.

Results

Elevated levels of chromatin-bound PCNA (via *elg1Δ*) promote cohesin binding to DNA in *mcd1* mutant cells

PCNA^{OE} (*POL30* expressed from a 2μ vector) and *elg1Δ*, both of which result in persistent and increased levels of chromatin-bound PCNA, adversely affect all core cohesin mutant strains tested to date [15, 32, 33, 35, 61, 63]. For instance, *mcd1-1* mutant cells are inviable at the restrictive temperature of 37°C, due to both high cohesion and condensation defects [1, 2], but lose viability at 34°C in response to either PCNA^{OE} or *elg1Δ* [32, 33]. Given that cohesin deposition onto chromatin and cycles of PCNA binding/release are normally coordinated [10, 21, 36], it became important to test whether elevated levels of chromatin-bound PCNA reduce cohesin deposition onto DNA—either through direct competition, reduction of factors that promote cohesin deposition (*Scs2,4*, *RSC* or *Chl1*), or increase in factors (*Rad61/WAPL*) that dissociate cohesin from chromatin [7, 8, 23, 30, 31, 63, 66–70]. We first independently verified the antagonistic effect that *elg1Δ* imparts on cells harboring *mcd1-1* mutations and indeed found severely exacerbated growth defects (Fig 1A). Next, we validated the efficiency of the Triton X-100-based fractionation procedure [3, 45]. We obtained clear separation of soluble components (using the cytoplasmic factor Phosphoglycerokinase—PGK) from those of chromatin-bound components (Histone 2B) (65). Finally, we optimized Western blot procedures to obtain a linear range of band intensities from which to quantify levels of fractionated chromatin-bound proteins (Fig 1B). To test whether elevated levels of chromatin-bound PCNA reduce cohesin binding to DNA, wildtype, *elg1Δ* and *mcd1-1* single mutant cells, and *mcd1-1 elg1Δ* double mutant cells, all of which express *Smc3-3V5* as the sole source of *Smc3* protein, were synchronized in G1 and released at either 34°C (the non-permissive temperature for *mcd1-1 elg1Δ* double mutant cells) or 37°C (the non-permissive temperature for *mcd1-1* single mutant cells) in fresh medium containing nocodazole. Cell cycle synchronizations were monitored by flow cytometry (Fig 1C). The resulting pre-anaphase cells were lysed and fractionated prior to assessing for changes in chromatin-bound *Smc3*, a core component of the cohesin complex [2, 71]. As expected, wildtype and *elg1Δ* single mutant cells display similar levels of chromatin bound *Smc3*, compared to H2B (Fig 1D and 1E). The results further reveal that *mcd1-1* single mutant cells display similar levels of chromatin-bound *Smc3* compared to wildtype cells, even at the non-permissive temperature of 37° (Fig 1D and 1E). Thus, *Mcd1* inactivation, which results in cell inviability, cohesion and condensation defects [1, 2], does so in the absence of cohesin dissociation from DNA (Fig 1D and 1E). Surprisingly, *mcd1-1 elg1Δ* double mutant cells display increased levels of chromatin bound cohesin at both non-permissive temperatures of 34° and 37°, compared to that of either wildtype, *elg1Δ* or *mcd1-1* single mutant cells (Fig 1D and 1E). These results that chromatin-bound levels of *Smc3* are not reduced in *mcd1-1 elg1Δ* double mutant cells, but instead are increased, reveal that excess chromatin-bound PCNA does not adversely impact cohesin loading onto DNA and negates both direct

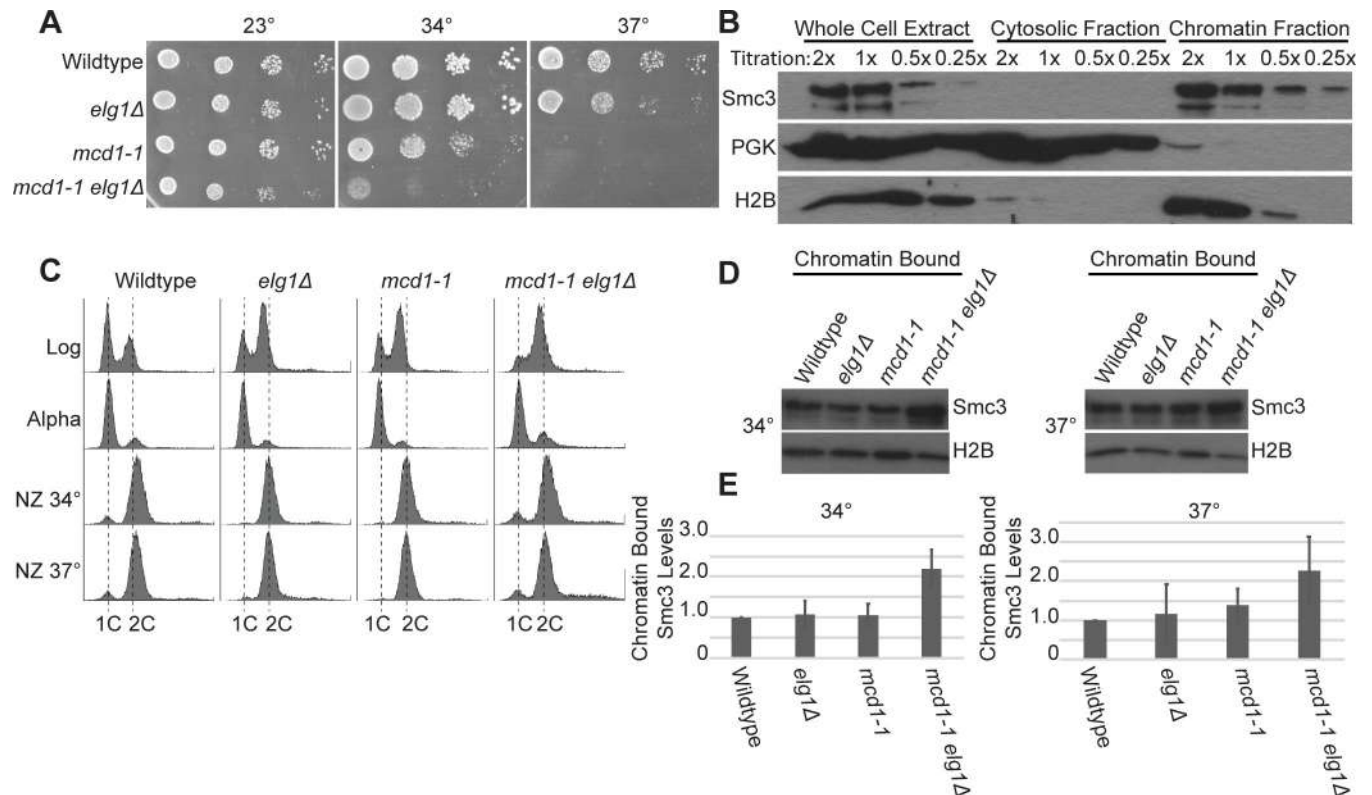


Fig 1. Excess chromatin-bound PCNA (via *elg1Δ*) increases cohesin chromatin levels in *mcd1* mutant cells. [A] 10-fold serial dilution of indicated yeast strains plated on rich medium plates and incubated at 23°C, 34°C, and 37°C for 2 days. [B] Titration and chromatin fractionation of wildtype cells arrested in nocodazole. 1X sample concentration for Smc3, H2B, and PGK indicates samples are within the linear range of detection. [C] DNA content of cells synchronized in G1 with alpha factor, and then shifted to 34°C or 37°C and arrested in pre-anaphase with nocodazole (NZ). [D] Chromatin bound fraction of cells arrested in pre-anaphase. Smc3 and H2B indicate levels of chromatin-bound proteins in the chromatin fraction. [E] Quantification of chromatin bound Smc3 levels, compared to H2B, in the indicated strains. Smc3 enrichment on DNA is based on the ratio of Smc3 to Histone 2B levels and obtained from 3 independent experiments. Error bars represent standard deviation.

<https://doi.org/10.1371/journal.pone.0235103.g001>

competition models and recruitment of cohesin releasing factors. The mechanism through which PCNA promotes cohesin deposition onto DNA remains an important issue in chromatin regulation.

Elevated levels of chromatin-bound PCNA (via *elg1Δ*) promote Smc3 acetylation in *mcd1* mutant cells

If excess levels of chromatin-bound PCNA (via *elg1Δ*) do not reduce cohesin deposition, PCNA may instead negatively impact acetylation of impaired cohesin to produce the observed cell growth defects. To test this possibility, wildtype, *elg1Δ* and *mcd1-1* single mutant cells, and *mcd1-1 elg1Δ* double mutant cells, all of which express Smc3-3V5 as the sole source of Smc3 function, were synchronized in G1 and released at 34°C or 37°C into fresh medium supplemented with nocodazole (Fig 2A). Protein samples were then assessed for Smc3 acetylation. Wildtype cells and *elg1Δ* single mutant cells contained similar levels of Smc3 acetylation at both temperatures. In contrast, *mcd1-1* single mutant cells exhibited a dramatic decrease in Smc3 acetylation at both temperatures (Fig 2B), despite the retention of both *mcd1-1* and Smc3 proteins on DNA (Fig 1E). This provides the first evidence that Mcd1 is critical for Eco1-dependent Smc3 acetylation and thus defines a new role for Mcd1 in promoting cohesin establishment. Importantly, *mcd1-1 elg1Δ* double mutant cells contained increased levels

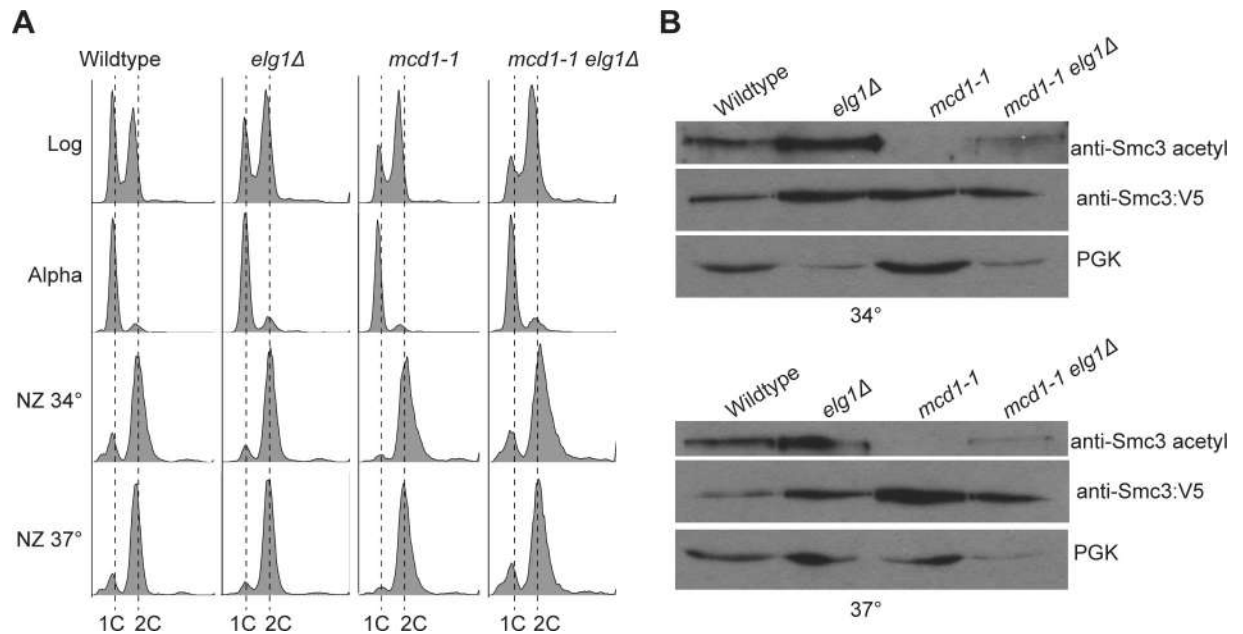


Fig 2. Excess chromatin bound PCNA (via *elg1Δ*) promotes Smc3 acetylation in *mcd1-1* mutant cells. [A] DNA content of log phase cells synchronized in G1, then shifted to 34°C or 37°C and arrested in pre-anaphase. [B] Elevated levels of chromatin-bound PCNA promotes Smc3 acetylation in *mcd1-1* mutant cells. Smc3 was detected by a V5 specific antibody, and acetylated Smc3 was detected by a K112/K113 acetylation antibody. PGK was used as a loading control.

<https://doi.org/10.1371/journal.pone.0235103.g002>

of Smc3 acetylation compared to *mcd1-1* single mutant cells, regardless of a temperature shift to either 34°C or 37°C (Fig 2B, S1 Fig), consistent with prior evidence that elevated levels of PCNA promote both *eco1* mutant cell viability and Eco1-dependent acetylation of Smc3 [10, 15]. In combination, these results reveal that elevated levels of chromatin-bound PCNA, via *elg1Δ*, do not negatively impact either binding or acetylation of cohesin. That elevated levels of chromatin-bound PCNA promotes both the acetylation and deposition of mutant cohesin therefore suggests that the adverse effect of PCNA occurs through some other mechanism.

Elevated levels of chromatin-bound PCNA (via 2μ *POL30*) increases *mcd1* mutant cell sensitivity to DNA damage agents

Given the exclusion of models in which elevated levels of chromatin-bound PCNA (via *elg1Δ*) reduce either cohesin binding to DNA or acetylation, we next hypothesized that PCNA-dependent growth defects of cohesin mutants might involve genomic instability. For instance, it is now well documented that very high levels of PCNA, obtained by *GAL*-based overexpression, renders wildtype cells hypersensitive to genotoxic agents and promotes elevated levels of sister chromatid recombination [63], phenotypes similarly exhibited by *elg1Δ* cells [60, 63, 72–74]. In contrast, studies involving relatively moderate increased levels of PCNA, via 2μ plasmids, have thus far failed to produce overt growth defects in wildtype cells [10, 15, 58, 63, 75]. We utilized this same 2μ plasmid strategy to ascertain whether a modest increase of chromatin-bound PCNA produces increased sensitivity to genotoxic agents in the context of cohesin mutant cells. Serial dilutions of wildtype and *mcd1-1* mutant cells harboring either *CEN* vector alone or 2μ vector containing *POL30* (PCNA) were plated on selective media supplemented with increasing concentrations of MMS, and maintained at the permissive temperature of 23°C. Wildtype cells, with or without the 2μ *POL30* plasmid, exhibited similar dose-dependent growth defects, but remained viable even at elevated levels of MMS (Fig 3A). *mcd1-1* single

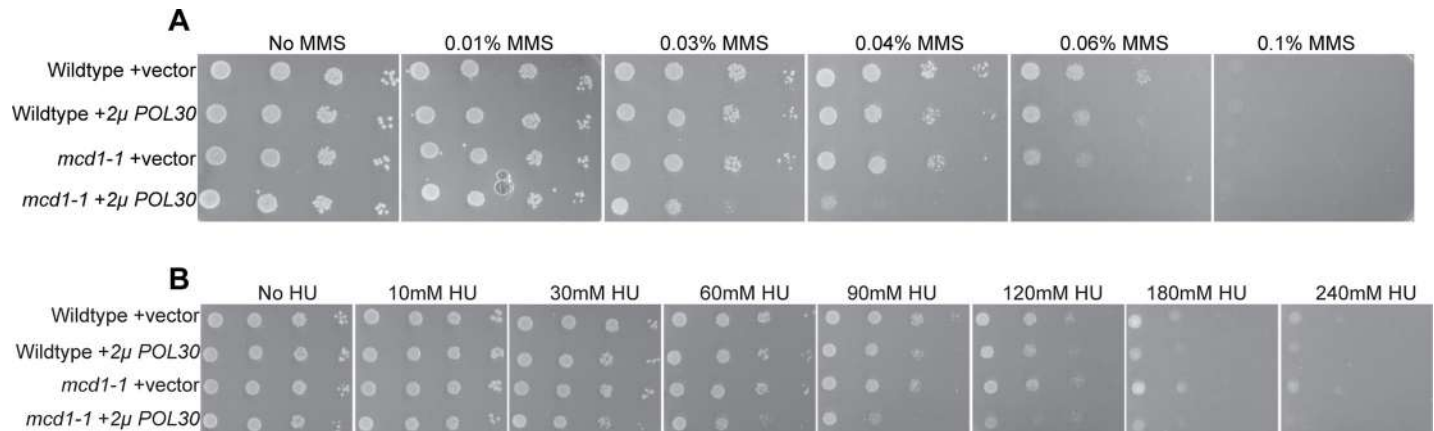


Fig 3. Elevated PCNA levels (via PCNA^{OE}) causes DNA damage sensitivity in *mcd1-1* mutant cells. [A] 10-fold serial dilution of indicated yeast strains plated on selective medium plates containing no MMS, 0.01% MMS, 0.03% MMS, 0.04% MMS, 0.06% MMS, or 0.1% MMS, and incubated at 23°C for 3 days. [B] 10-fold serial dilution of indicated yeast strains plated on selective medium plates containing no HU, 10mM HU, 30mM HU, 60mM HU, 90mM HU, 120mM HU, 180mM HU, or 240mM HU, and incubated at 23°C for 3 days.

<https://doi.org/10.1371/journal.pone.0235103.g003>

mutant cells that harbored the vector alone exhibited growth rates nearly identical to those of wildtype cells across the entire dose range of MMS. In contrast, *mcd1-1* mutant cells that harbored the 2μ *POL30* plasmid (PCNA^{OE}) produced significant growth defects that coincided with increased MMS levels (Fig 3A). In combination, this result suggests that even moderate PCNA^{OE} adversely impacts genomic integrity, but an effect which is detected here only in cohesin mutant cells sensitized by MMS.

We next tested whether this moderate PCNA^{OE} is sufficient to sensitize *mcd1-1* mutant cells to replication fork destabilizing agents. Hydroxyurea (HU) inhibits RNR function, resulting in depletion of dNTPs and destabilized DNA replication forks [76]. Serial dilutions of wildtype and *mcd1-1* mutant cells, harboring either *CEN* vector alone or with 2μ *POL30*, were exposed to various concentrations of HU and maintained at the permissive temperature of 23°C. Wildtype cells, with or without elevated PCNA levels, were largely refractile to HU except at the most extreme concentration of HU, at which PCNA produced a minor growth defect (Fig 3B). Interestingly, *mcd1-1* mutant cells that harbor the vector alone exhibited growth comparable to that of wildtype cells at all concentrations of HU. *mcd1-1* mutant cells that harbor 2μ *POL30* plasmid, however, exhibited significant growth defects even at relatively moderate levels of HU (Fig 3B). To assess the effect of elevated levels of chromatin-bound PCNA, in the absence of increased cytosolic levels of PCNA, we also tested the combined effects of *elg1Δ* and DNA damaging agents on wildtype and *mcd1-1* mutant cells. Similar to results obtained from PCNA^{OE}, the deletion of *EGL1* from *mcd1-1* cells produced extreme sensitivities to both MMS and HU (S2 Fig). These results are consistent with prior studies that cohesin plays a critical role in stalled replication fork restart as well as DNA damage repair [77–80].

Elevated levels of chromatin-bound PCNA (via 2μ *POL30*) activate the Mec1/ATR DNA damage response pathway and impact cell cycle progression

The adverse effect of 2μ *POL30* and *elg1Δ* on *mcd1-1* mutant cells is consistent with the model that even very moderate levels of PCNA is detrimental to genome maintenance. Mec1 (ATR) and Tel1 (ATM) kinases form parallel DNA damage response pathways [81–84]. To determine

which, if either, pathway responds to PCNA^{OE}, *tel1Δ1* and *mec1-1* mutant cells were transformed with a CEN vector alone or *2μ* vector with *POL30* and grown on plates maintained at a range of temperatures. Surprisingly, neither *tel1Δ1* nor *mec1-1* mutant cells exhibited any adverse growth rates in response to PCNA^{OE}, regardless of the temperature (Fig 4A). We next assessed if either *tel1Δ1* or *mec1-1* mutant cells, sensitized by low doses of MMS, might reveal adverse effects of PCNA^{OE}. *tel1Δ1* mutant cells that harbor the *2μ POL30* plasmid exhibited growth nearly identical to that of wildtype cells, despite the presence of MMS. Conversely, *mec1-1* mutant cells that harbor the *2μ POL30* plasmid exhibited significant growth defects in the presence of MMS (Fig 4B).

Phosphorylation of the DNA damage checkpoint kinase Rad53 occurs in a Mec1-dependent manner [85]. Rad53 is not phosphorylated in cells depleted of Elg1 under normal conditions, even though this checkpoint pathway is competent to respond to genotoxic agents [21, 61, 73]. These studies suggest that *mcd1-1 elg1Δ* double mutant cells would similarly not exhibit elevated Rad53 phosphorylation, despite the exacerbated growth defect at the restrictive temperature. To test this prediction, wildtype, both *mcd1-1* and *elg1Δ* single mutants, and *mcd1-1 elg1Δ* double mutant cells were synchronized in G1, washed, and released in nocodazole at 37°C. As a positive control, wildtype cell cultures were split in two, with one population exposed to 0.05% MMS, prior to assessing for Rad53 phosphorylation in all strains. As expected, Rad53 exhibited a clear upward shift in wildtype cells exposed to 0.05% MMS, compared to Rad53 obtained from untreated wildtype and *elg1Δ* single mutant cells, consistent with prior results [61]. Interestingly, neither *mcd1-1* single mutant nor *mcd1-1 elg1Δ* double mutant cells exhibited a shift in Rad53 migration (Fig 4C). These results suggest that increased levels of chromatin-bound PCNA generates genomic instabilities that can activate a Mec1/ATR (but not Tel1/ATM) DNA damage repair pathway but in the absence of Rad53 phosphorylation.

PCNA^{OE} sensitizes *mcd1-1* mutant cells to MMS and HU and also activates the Mec1/ATR intra-S phase checkpoint, suggesting that elevated PCNA levels may adversely impact replication fork progression. Consistent with this hypothesis, mutation of either *ESCO2* (human homolog of yeast *ECO1*) or cohesin subunits result in slowed fork progression in mammalian cells [86–89], although a velocity reduction appears absent in analogous yeast mutant strains [2, 3, 10, 77, 80, 90–92]. It thus became important to test whether elevated levels of chromatin-bound PCNA produces replication stress severe enough to delay S phase progression in *mcd1-1* mutant cells. Log phase wildtype, both *elg1Δ* and *mcd1-1* single mutant cells, and *mcd1-1 elg1Δ* double mutant cells were synchronized in G1, washed, and released into fresh medium supplemented with nocodazole and maintained at the either 32° (restrictive temperature for *mcd1-1 elg1Δ* double mutant cells) or 37°C (restrictive temperature for *mcd1-1* single mutant cells). Aliquots were harvested at 15 minute intervals and cell cycle progression monitored by flow cytometry (S3 Fig). Because cells harboring *ELG1* deletion do not fully synchronize in G1 with alpha factor [32], we analyzed the time point at which at least half of a G1 arrested population progressed to an S-phase state. At 32°C, wildtype and *elg1Δ* mutant cells both reached a half-way point (relatively equal 1N and 2N peaks) between the 30–45 minute time points, while arresting in pre-anaphase in about 75 minutes. *mcd1-1* mutant cells progressed to a mid-way state at the tail end of the time range (45 minutes) required by wildtype and *elg1Δ* mutant cells, and achieved a final preanaphase state in coordination with wildtype and *elg1Δ* mutant cells. At 37°C, which is non-permissive for both *mcd1-1* and *mcd1-1 elg1Δ* mutant cells, *mcd1-1* cells are clearly delayed by almost two time points in progressing to a half-way state (75 minutes), compared to wildtype and *elg1Δ* mutant cells (45–60 minutes) and delayed by a full time point in achieving a preanaphase arrest (90 minutes in *mcd1-1* cells compared to 75 minutes in both wildtype and *elg1Δ* cells). Interestingly, *mcd1-1 elg1Δ* double mutant cells instead both exit

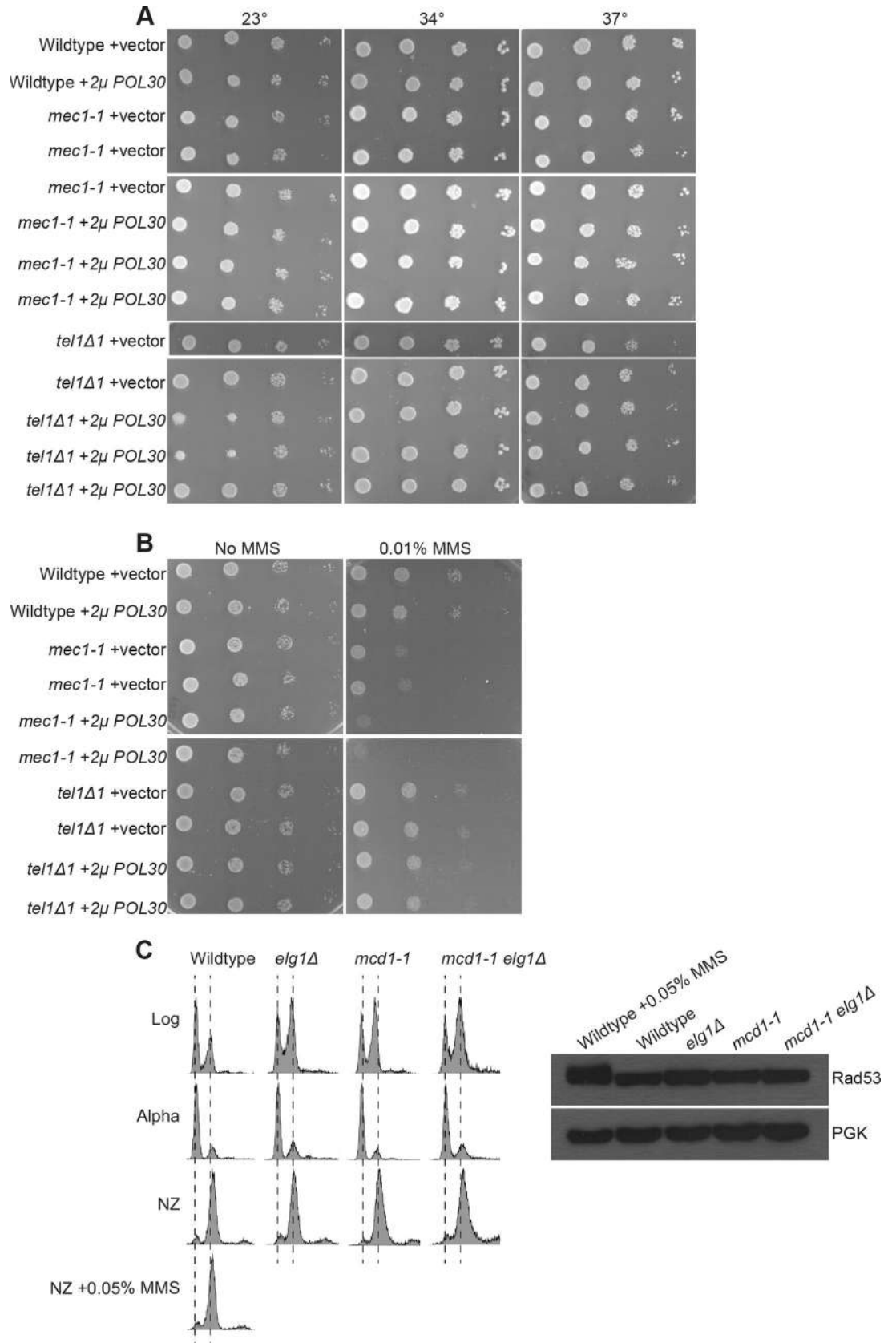


Fig 4. Elevated levels of PCNA sensitizes *mec1-1* mutant cells to MMS. [A] Elevated levels of PCNA does not impact *tel1Δ1* and *mec1-1* mutant cells under high temperature stress. 10-fold serial dilution of indicated yeast strains plated on selective medium plates and incubated at 23°C, 34°C, and 37°C for 2 days. [B] Elevated levels of PCNA specifically sensitizes *mec1-1* mutant cells when exposed to DNA damage. 10-fold serial dilution of indicated yeast strains plated on selective medium plates containing no MMS or 0.01% MMS and incubated at 23°C for 2 days. [C] Rad53 checkpoint is not activated in *mcd1-1 elg1Δ* double mutant cells. DNA content are shown for cells in log phase, synchronized in G1 with alpha factor, and released and shifted to 37°C and arrested in pre-anaphase. Wildtype cells exposed to 0.05% MMS was used as a positive control for Rad53 activation. Rad53 was detected using a Rad53 specific antibody, and PGK was used as a loading control.

<https://doi.org/10.1371/journal.pone.0235103.g004>

G1 and achieve a mid-way state (15 minutes) faster than all other strains at both 32°C and 37°C, but then remain in this mid-way state for an extended period of time of 30 minutes (15–45 minutes) at 37°C, relative to other strains (S3 Fig). These results suggest that elevated levels of chromatin-bound PCNA, in combination with cohesin mutation, adversely impacts replication fork progression.

The differential impacts of PCNA^{OE} on various cohesin mutant cells

High levels of PCNA (*GAL*-dependent *POL30* overexpression) results in phenotypes that overlap with those obtained by *elg1Δ*, although *elg1Δ* phenotypes are far more robust [63, 73, 74, 93]. It thus became important to ascertain the effect of *elg1Δ* on cohesin mutants to that of a moderate increase (2 μ -based) in PCNA levels. Our results document that, not only *mcd1-1* cells, but also *smc1-259* and *smc3-42* mutant cells exhibit growth defects in response to *elg1Δ* (Fig 5A), consistent with prior studies [33, 35]. We next tested whether wildtype PCNA (via 2 μ plasmid) would similarly exacerbate cohesin mutant cell growth. The results reveal that PCNA^{OE} severely exacerbates the temperature sensitivity of *mcd1-1* mutant cells (Fig 5B), consistent with a previous study [15]. Surprisingly, PCNA^{OE} exhibited no adverse effect on either *smc1-259* or *smc3-42* mutant cell growth (Fig 5B). We repeated our analysis on different cohesin alleles. The results show that PCNA^{OE} similarly failed to adversely impact the growth of *smc1-2* and *smc3-5* mutant cells. At first blush, these results appear in stark contrast to those reported by Zhang and colleagues for both *smc1-259* and *smc3-42* mutant cell [15]. Our results, however, are predicated on PCNA expressed from the endogenous promoter in which elevated expression is driven solely by the multi-copy 2 μ plasmid [10]. In contrast, the Zhang study expressed PCNA using the constitutive and high-expressing ADH promoter in the context of the high copy 2 μ plasmid (pGADT7), suggesting that the two results may differ due to PCNA expression levels. To test this hypothesis, we cloned *POL30* into pGADT7. The resulting PCNA construct, however, produced a dominant-negative phenotype such that all strains tested, including wildtype cells, exhibited severe growth defects (Fig 5C). We confirmed that both overexpressed PCNA from the multi-copy 2 μ plasmid and high copy 2 μ plasmid (pGADT7) resulted in elevated levels of chromatin-bound PCNA (Fig 5D–5F and S4 Fig). Therefore, it is possible that this dominant-negative effect is due to elevated levels of epitope-tagged PCNA as occurs for pGADT7 tagging which is absent in our 2 μ strategy. Prior studies, for instance, document that endogenous expression of either N- and C-terminus tagged PCNA can result in wildtype cell increased MMS sensitivity [62, 75]. Regardless, our results reveal that *mcd1-1*, in contrast to numerous other cohesin subunit alleles (which exhibit similar conditional growth defects—Fig 5), are hypersensitive to even a moderate increase in wildtype PCNA.

Discussion

Since the first evidence that cohesion establishment is intimately coupled to DNA replication [10], a wealth of studies document the dependency of Eco1 recruitment by DNA replication

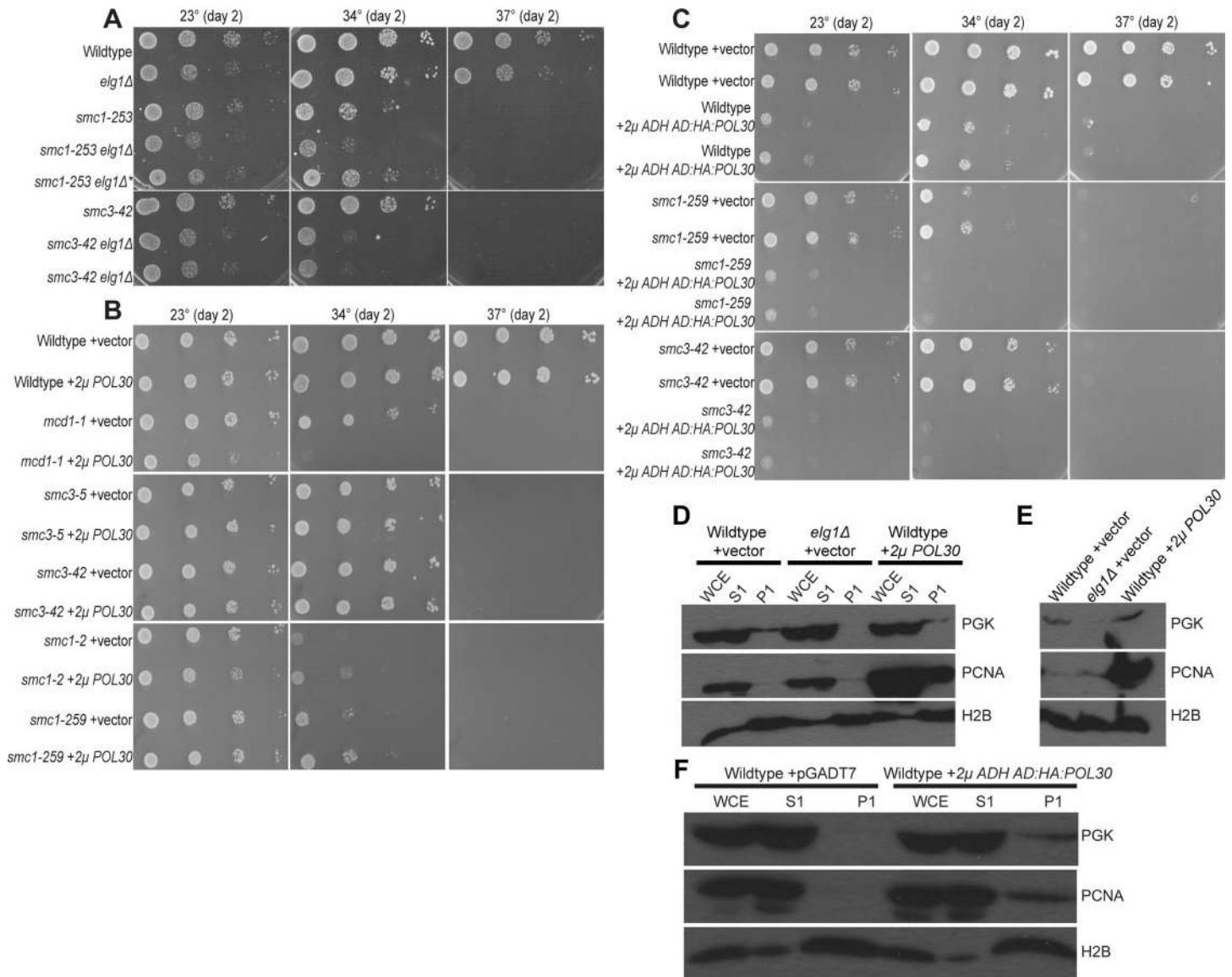


Fig 5. Elevated levels of chromatin-bound PCNA differentially impacts cohesin alleles. [A] *ELG1* deletion exacerbates *smc1-259* and *smc3-42* mutant cells. 10-fold serial dilution of indicated yeast strains plated on rich medium plates and incubated at 23°C, 34°C, and 37°C for 2 days. * indicates a mutated *smc1-259 elg1Δ* strain that displays a resistant to temperature sensitivity [B] PCNA^{OE} from a 2 μ plasmid specifically impacts *mcd1-1* mutant cells. 10-fold serial dilution of indicated yeast strains plated on selective medium plates and incubated at 23°C, 34°C, and 37°C for 2 days. [C] Overexpressed PCNA harboring a GAL4 AD and HA N-terminal tag exacerbates cell growth in wildtype cells, *smc1-259*, and *smc3-42* mutant cells. Images of *POL30* in pGADT7 in WT, *smc3-42*, and *smc1-259* mutant cells. 10-fold serial dilution of indicated yeast strains plated on selective medium plates and incubated at 23°C, 34°C, and 37°C for 2 days. [D] Log phase wildtype cells that harbor 2 μ *POL30* plasmid produce elevated levels of chromatin-bound PCNA, compared to wildtype cells that harbor a vector plasmid and *elg1Δ* single mutant cells. PGK and H2B were used as a loading control and control for chromatin fractionation, respectively. [E] Five times the chromatin fraction of Fig 5D was loaded to visualize chromatin-bound PCNA in wildtype cells. [F] Overexpressed PCNA via a high copy 2 μ plasmid in log phase wildtype cells results in elevated levels of chromatin-bound PCNA compared to log phase wildtype cells harboring a vector plasmid. PCNA was detected by a PCNA specific antibody. PGK and H2B was used as a loading control and control for chromatin fractionation.

<https://doi.org/10.1371/journal.pone.0235103.g005>

fork factors and, furthermore, that replication fork factors regulate sister chromatid tethering reactions [14, 15, 23–25, 29, 32, 33, 35, 36, 94–98]. Of particular interest are RFC complexes that regulate the loading (RFC1^{RF}, Ctf18^{RF}) and unloading (Elg1^{RF}) of PCNA onto DNA [61, 99–101]. Either PCNA overexpression or *ELG1* deletion, both of which result in prolonged and elevated retention of PCNA onto DNA, rescue *eco1* mutant cell growth [10, 15, 32,

33]. Intriguingly, however, elevated levels of chromatin-bound PCNA instead exacerbates the growth defects of the cohesin subunits [15, 33], a surprising phenotype given that the cohesin subunit Smc3 is the target of Eco1 acetylation [12, 13, 102]. *ELG1* deletion is mutagenic and thus may have adverse impacts beyond PCNA unloading while moderate increases in PCNA appear fully tolerated by wildtype cells [58, 60, 63, 73, 75, 103]. Here, we confirm that *ELG1* deletion exacerbates the growth defects present in *mcd1* mutant cells and extend those findings to show that moderate overexpression of wildtype PCNA similarly exerts an adverse growth effect on *mcd1* mutant cell growth. The link between PCNA and cohesin function is complex, however, in that similar expression of PCNA had no impact on a number of other cohesin subunit alleles (*smc3-5*, *smc3-42*, *smc1-295* and *smc1-2*). These findings raise the possibility that cohesin loading onto sister chromatids, which occurs behind DNA polymerase and PCNA [10, 21, 36], may be oriented such that Mcd1 is most proximal to, and thus most impacted by, DNA replication fork components. Interestingly, deletion of *ELG1* (PCNA-unloader), and independent deletion of *CTF18* (PCNA-loader), both exacerbate cohesin mutant cell growth [10, 102]. While our current study was under review, recent findings revealed that dual deletion of *ELG1* and *CTF18* returns to near-normal both chromatin-bound PCNA and cohesion levels, with additional evidence for strand-specific RFC roles in PCNA deposition [21]. Thus, cohesin function is negatively impacted by altering both PCNA dynamics, in either direction, and residency. Additional studies are required to elucidate the multiple mechanisms through which DNA replication fork components, especially involving PCNA, impact cohesin functions.

A second major finding from this study are surprising impacts of elevated levels of chromatin-bound wildtype PCNA on cohesin regulation. Elevated levels of chromatin-bound PCNA that persist well after S phase could antagonize any number of post-replicative activities such as histone deposition, chromatin remodeling, or Okazaki maturation [104, 105]. Given the adverse impact of elevated levels of chromatin-bound PCNA on *mcd1-1* mutant cells, PCNA might conceivably reduce Scc2, Scc4 recruitment and/or subsequent deposition of cohesins onto DNA [8, 23, 66, 106, 107]. An alternate model is that elevated levels of PCNA sequester Eco1 into soluble PCNA pools, precluding sufficient cohesin acetylation. We provide evidence that negate both of these models. Our finding reveals that mutant *mcd1* impedes Smc3 acetylation, a new observation that suggests that Mcd1 supports Eco1-dependent acetylation in a manner yet unknown. Furthermore, our study supports prior findings that elevated chromatin-binding of PCNA improves Smc3 acetylation [10, 15, 21]. More importantly, the finding that increased PCNA promotes cohesin binding onto DNA suggests that factors that promote cohesin deposition (Scc2,4, Chl1, or RSC), or promote cohesin dissociation (Rad61), are themselves sensitive to PCNA levels or modifications [8, 23, 24, 59, 98]. In support of this model are reports that PCNA physically interacts with Chl1, which promotes the recruitment to DNA of both Scc2,4 and cohesin [14, 23, 66, 107]. Intriguingly, increased Smc3 acetylation and cohesin deposition, induced by *elg1Δ*, fails to rescue *mcd1-1* mutant cell growth defects, suggesting that PCNA impacts cohesin functions beyond sister chromatid tethering pathways—as described below.

A third major finding from the current study involves identifying potential mechanisms through which PCNA renders *mcd1-1* mutant cells inviable. It is well known that *elg1Δ* results in long-lived and elevated levels of chromatin-bound PCNA which is highly mutagenic to wildtype cells [73, 74, 93]. High levels of PCNA, achieved by *GAL*-overexpression or coupling *ADH*-overexpression to 2μ -based high copy number, similarly produce genomic instabilities [15, 63]. A much more moderate expression system (2μ high copy) has thus far shown no adverse effect in wildtype cells [10, 58]. Our findings document that PCNA^{OE} is sufficient to produce growth defects in *mcd1-1* mutant cells, and that this effect is greatly exacerbated by

challenging mutant cells with MMS or HU. This intersection between PCNA and cohesin is consistent with prior studies that document that 1) highly elevated levels of PCNA result in genomic instability [63], 2) cohesin are both recruited to stalled replication forks and promote fork restart [77–79, 89], and 3) DNA replication fork protection complexes and cohesin pathways are intimately linked [24, 63, 77, 80, 108]. During the final stages of this study, independent analyses revealed that elevated levels of chromatin-bound PCNA results in hyper-recruitment of mismatch repair factors [109]. Cells that exhibit elevated levels of mismatch repair intermediates normally activate cohesin recruitment pathways to promote efficient DNA repair through homologous recombination [110, 111]. Cells utilize Msh2-Msh3-dependent mismatch repair (MMR) to correct mismatches (including short insertions and deletions) that accumulate during DNA replication [109, 112–114], which increase upon high levels of PCNA expression [109]. However, numerous *mcd1-1 msh3Δ elg1Δ* triple mutant cells were obtained from crossing *msh3Δ* single mutant cells to *mcd1-1 elg1Δ* double mutant cells (S4 Table). Thus, the moderate increase of PCNA used here does not appear to generate long-lived genomic instabilities sufficient to require mismatch repair factor Msh3. Despite this, our findings document that the adverse effect of PCNA^{OE} does result in a Mec1(ATR)-dependent response, versus a Tel1(ATM)-dependent response, but in the absence of Rad53 phosphorylation. The integration of Mec1 sensor in PCNA and cohesin genome instability contrasts those in which double deletion of *MEC1* and *TEL1* were required to reduce Scc1 recruitment to forks under conditions of replication stress [77]. In combination, these findings highlight the complex nature through which Mec1 (and possibly Tel1) respond to replication stressors (such as PCNA^{OE}), which are revealed only under conditions of cohesin mutation and/or genotoxic agents.

A confluence of findings document that 1) cohesins are deposited during S phase onto nascent sister chromatids [8, 10, 65, 115–120], 2) cohesins are critical for replication fork

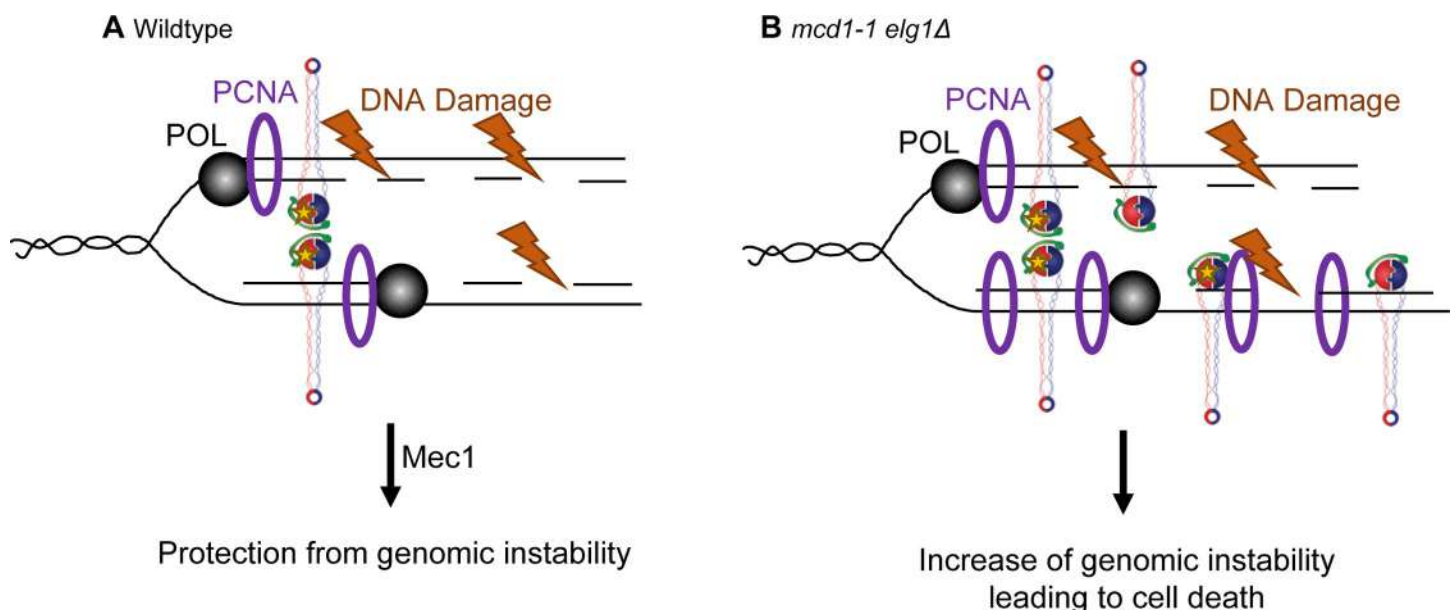


Fig 6. Cohesins are necessary to resolve genomic instabilities caused by elevated levels of PCNA. [A] In wildtype cells, a functional Elg1 removes PCNA from behind the replication fork. If DNA damage occurs, the damage is resolved in a Mec1-dependent manner. Proper DNA repair and protection from genomic instability results in cell viability. [B]. In *mcd1-1 elg1Δ* double mutant cells, loss of Elg1 results in the retention of chromatin-bound PCNA. The combination of misregulated PCNA and a mutant cohesin (which exhibits reduced acetylation) may result in unrepaired DNA and unresolved genomic stability, leading to cell death.

<https://doi.org/10.1371/journal.pone.0235103.g006>

restart and repair [77–79, 88], 3) Eco1-dependent cohesin establishment is intimately coupled to PCNA and the DNA replication fork [10, 15, 16, 25–27, 121–123], and 4) PCNA^{OE} and *elg1Δ* both adversely impact cohesin mutant cell growth. Clearly, PCNA^{OE} (at even very moderate levels) and *elg1Δ* adversely impact cohesin mutant cell growth, an effect exacerbated by genotoxic agents. We thus posit a model that may explain why elevated levels of PCNA reduce *mcd1-1* mutant cell growth (Fig 6). In wildtype cells, PCNA is removed from chromatin by Elg1 and proper cohesin deposition and acetylation occur to establish sister chromatid cohesion. Elevated levels of chromatin-bound PCNA result in minor genomic instabilities that likely impact replication fork progression, but at a level insufficient for Mec1 to promote Rad53 phosphorylation. Cohesin mutant cells are unable to counter the adverse effects of PCNA—which eventually leads to cell death.

Supporting information

S1 Fig. Elevated levels of PCNA promote Eco1-dependent cohesin acetylation. Second biological iteration of Fig 2. Smc3 was detected by a V5 specific antibody, and acetylated Smc3 was detected by a K112/K113 acetylation antibody. PGK was used as a loading control. (PDF)

S2 Fig. Elevated chromatin-bound PCNA (via *elg1Δ*) causes DNA damage sensitivity in *mcd1-1* mutant cells. [A] 10-fold serial dilution of indicated yeast strains plated on selective medium plates containing no MMS, 0.03% MMS, 0.06% MMS, or 0.1% MMS, and incubated at 23°C for 3 days. [B] 10-fold serial dilution of indicated yeast strains plated on selective medium plates containing no HU, 60mM HU, 120mM HU, or 240mM HU, and incubated at 23°C for 3 days. (PDF)

S3 Fig. Excess chromatin bound PCNA does not cause a S-phase checkpoint activation in wildtype or *mcd1-1* mutant cells. DNA content of log phase cells synchronized in G1. Temperature was then shifted to either 32°C or 37°C and cells released into media supplemented with nocodazole. Samples were collected every 15 minutes. (PDF)

S4 Fig. PCNA overexpressed from a multi-copy 2μ plasmid and a high copy 2μ plasmid results in elevated levels of chromatin-bound PCNA. [A] Second biological replicate of Fig 5D. Wildtype cells harboring a 2μ *POL30* plasmid results in elevated levels of chromatin-bound PCNA compared to wildtype cells harboring a vector plasmid and *elg1Δ* single mutant cells. PCNA was detected by a PCNA specific antibody. PGK and H2B was used as a loading control and control for chromatin fractionation. [B] Five times the chromatin fraction was loaded to visualize chromatin-bound PCNA in wildtype cells. [C] Second biological replicate of Fig 5F. Overexpressed PCNA via a high copy 2μ plasmid results in elevated levels of chromatin-bound PCNA compared to wildtype cells harboring a vector plasmid. PCNA was detected by a PCNA specific antibody. PGK and H2B was used as a loading control and control for chromatin fractionation. (PDF)

S1 Table. Reagents used in this study.
(DOCX)

S2 Table. Strains used in this study.
(DOCX)

S3 Table. Plasmids used in this study.

(DOCX)

S4 Table. *msh3Δ* does not result in cell spore lethality in *mcd1-1 elg1Δ* double mutant cells.

Dissection of *mcd1-1 elg1Δ Smc3:3V5* mated with *msh3Δ*. *mcd1-1 elg1Δ msh3Δ* triple mutant strains are obtained at the expected frequency.

(DOCX)

Acknowledgments

We thank the R.V.S. laboratory members (Michael Mfarej, Annie Sanchez, Nicole Kirven, and Shaya Ameri) for helpful comments during the progression of this study. We also thank Dr. Vincent Guacci, Dr. Douglas Koshland, Dr. Gregory Lang, and Dr. Katsuhiko Shirahige for generously sharing yeast strains and reagents. Any opinions, findings, and conclusions or recommendations expressed in this study are those of the authors and does not necessarily reflect the views of the National Institutes of Health. No competing interests are declared.

Author Contributions

Conceptualization: Robert V. Skibbens.

Formal analysis: Caitlin M. Zuilkoski, Robert V. Skibbens.

Funding acquisition: Robert V. Skibbens.

Investigation: Caitlin M. Zuilkoski.

Methodology: Caitlin M. Zuilkoski.

Project administration: Caitlin M. Zuilkoski, Robert V. Skibbens.

Resources: Robert V. Skibbens.

Supervision: Robert V. Skibbens.

Validation: Caitlin M. Zuilkoski.

Writing – original draft: Caitlin M. Zuilkoski.

Writing – review & editing: Robert V. Skibbens.

References

1. Guacci V, Koshland D, Strunnikov A. A direct link between sister chromatid cohesion and chromosome condensation revealed through the analysis of MCD1 in *S. cerevisiae*. *Cell*. 1997; 91: 47–57. [https://doi.org/10.1016/s0092-8674\(01\)80008-8](https://doi.org/10.1016/s0092-8674(01)80008-8) PMID: 9335334
2. Michaelis C, Ciosk R, Nasmyth K. Cohesins: Chromosomal proteins that prevent premature separation of sister chromatids. *Cell*. 1997; 91: 35–45. [https://doi.org/10.1016/s0092-8674\(01\)80007-6](https://doi.org/10.1016/s0092-8674(01)80007-6) PMID: 9335333
3. Tóth A, Ciosk R, Uhlmann F, Galova M, Schleiffer A, Nasmyth K. Yeast cohesin complex requires a conserved protein, Eco1p(Ctf7), to establish cohesion between sister chromatids during DNA replication. *Genes Dev*. 1999; 13: 320–333. <https://doi.org/10.1101/gad.13.3.320> PMID: 9990856
4. Panizza S, Tanaka T, Hochwagen A, Eisenhaber F, Nasmyth K. Pds5 cooperates with cohesin in maintaining sister chromatid cohesion. *Curr Biol*. 2000; 10: 1557–1564. [https://doi.org/10.1016/s0960-9822\(00\)00854-x](https://doi.org/10.1016/s0960-9822(00)00854-x) PMID: 11137006
5. Hartman T, Stead K, Koshland D, Guacci V. Pds5p Is an Essential Chromosomal Protein Required for both Sister Chromatid Cohesion and Condensation in *Saccharomyces cerevisiae*. *J Cell Biol*. 2000; 151: 613–626. <https://doi.org/10.1083/jcb.151.3.613> PMID: 11062262

6. Rankin S, Ayad NG, Kirschner MW. Sororin, a substrate of the anaphase-promoting complex, is required for sister chromatid cohesion in vertebrates. *Mol Cell*. 2005; 18: 185–200. <https://doi.org/10.1016/j.molcel.2005.03.017> PMID: 15837422
7. Kueng S, Hegemann B, Peters BH, Lipp JJ, Schleiffer A, Mechtler K, et al. Wapl Controls the Dynamic Association of Cohesin with Chromatin. *Cell*. 2006; 127: 955–967. <https://doi.org/10.1016/j.cell.2006.09.040> PMID: 17113138
8. Ciosk R, Shirayama M, Shevchenko A, Tanaka T, Toth A, Shevchenko A, et al. Cohesin's binding to chromosomes depends on a separate complex consisting of Scc2 and Scc4 proteins. *Mol Cell*. 2000; 5: 243–254. [https://doi.org/10.1016/s1097-2765\(00\)80420-7](https://doi.org/10.1016/s1097-2765(00)80420-7) PMID: 10882066
9. Watrin E, Schleiffer A, Tanaka K, Eisenhaber F, Nasmyth K, Peters JM. Human Scc4 Is Required for Cohesin Binding to Chromatin, Sister-Chromatid Cohesion, and Mitotic Progression. *Curr Biol*. 2006; 16: 863–874. <https://doi.org/10.1016/j.cub.2006.03.049> PMID: 16682347
10. Skibbens R V, Corson LB, Koshland D, Hieter P. Ctf7p is essential for sister chromatid cohesion and links mitotic chromosome structure to the DNA replication machinery. *Genes Dev*. 1999; 13: 307–319. <https://doi.org/10.1101/gad.13.3.307> PMID: 9990855
11. Ivanov D, Schleiffer A, Eisenhaber F, Mechtler K, Haering CH, Nasmyth K. Eco1 is a novel acetyltransferase that can acetylate proteins involved in cohesion. *Curr Biol*. 2002; 12: 323–328. [https://doi.org/10.1016/s0960-9822\(02\)00681-4](https://doi.org/10.1016/s0960-9822(02)00681-4) PMID: 11864574
12. Rolef Ben-shahar T, Heeger S, Lehane C, East P, Flynn H, Skehel M, et al. Eco1-Dependent Cohesin Sister Chromatid Cohesion. *Science* (80-). 2008; 321: 563–566. <https://doi.org/10.1126/science.1157774> PMID: 18653893
13. Unal E, Heidinger-Pauli JM, Kim W, Guacci V, Onn I, Gygi SP, et al. A Molecular Determinant for the Establishment of Sister Chromatid Cohesion. *Science* (80-). 2008; 321: 566. <https://doi.org/10.1126/science.1172133> PMID: 19628857
14. Moldovan GL, Pfander B, Jentsch S. PCNA Controls Establishment of Sister Chromatid Cohesion during S Phase. *Mol Cell*. 2006; 23: 723–732. <https://doi.org/10.1016/j.molcel.2006.07.007> PMID: 16934511
15. Zhang J, Shi D, Li X, Ding L, Tang J, Liu C, et al. Rtt101-Mms1-Mms22 coordinates replication-coupled sister chromatid cohesion and nucleosome assembly. *EMBO Rep*. 2017; 18: 1294–1305. <https://doi.org/10.15252/embr.201643807> PMID: 28615292
16. Bender D, Da Silva EML, Chen J, Poss A, Gawey L, Rulon Z, et al. Multivalent interaction of ESCO2 with the replication machinery is required for cohesion. *Proc Natl Acad Sci*. 2020; 117: 1081–1089. <https://doi.org/10.1073/pnas.1911936117> PMID: 31879348
17. Ohashi E, Tsurimoto T. Functions of Multiple Clamp and Clamp-Loader Complexes in Eukaryotic DNA Replication. *Adv Exp Med Biol*. 2017; 1042: 135–162. https://doi.org/10.1007/978-981-10-6955-0_7 PMID: 29357057
18. Choe KN, Moldovan GL. Forging Ahead through Darkness: PCNA, Still the Principal Conductor at the Replication Fork. *Mol Cell*. 2017; 65: 380–392. <https://doi.org/10.1016/j.molcel.2016.12.020> PMID: 28157503
19. Leung W, Baxley RM, Moldovan G, Bielinsky A. Mechanisms of DNA Damage Tolerance: Post-Translational Regulation of PCNA. *Genes (Basel)*. 2019; 10. <https://doi.org/10.3390/genes10010010> PMID: 30586904
20. Slade D. Maneuvers on PCNA Rings during DNA Replication and Repair. *Genes (Basel)*. 2018; 9. <https://doi.org/10.3390/genes9080416> PMID: 30126151
21. Liu HW, Bouchoux C, Panarotto M, Kakui Y, Patel H, Uhlmann F. Division of Labor between PCNA Loaders in DNA Replication and Sister Chromatid Cohesion Establishment. *Mol Cell*. 2020; 78. <https://doi.org/10.1016/j.molcel.2020.03.017> PMID: 32277910
22. Hanna JS, Kroll ES, Lundblad V, Spencer FA. *Saccharomyces cerevisiae* CTF18 and CTF4 Are Required for Sister Chromatid Cohesion. *Mol Cell Biol*. 2001; 21: 3144–3158. <https://doi.org/10.1128/MCB.21.9.3144-3158.2001> PMID: 11287619
23. Rudra S, Skibbens R V. Chl1 DNA Helicase Regulates Scc2 Deposition Specifically during DNA-Replication in *Saccharomyces cerevisiae*. *PLoS One*. 2013; 8. <https://doi.org/10.1371/journal.pone.0075435> PMID: 24086532
24. Samora CP, Saksouk J, Goswami P, Wade BO, Singleton MR, Bates PA, et al. Ctf4 Links DNA Replication with Sister Chromatid Cohesion Establishment by Recruiting the Chl1 Helicase to the Replicosome. *Mol Cell*. 2016; 63: 371–384. <https://doi.org/10.1016/j.molcel.2016.05.036> PMID: 27397686
25. Zhang W, Yeung CHL, Wu L, Yuen KWY. E3 ubiquitin ligase Bre1 couples sister chromatid cohesion establishment to DNA replication in *Saccharomyces cerevisiae*. *Elife*. 2017; 6.

26. Ivanov MP, Ladurner R, Poser I, Beveridge R, Rampler E, Hudecz O, et al. The replicative helicase MCM recruits cohesin acetyltransferase ESCO2 to mediate centromeric sister chromatid cohesion. *EMBO J*. 2018; e97150. <https://doi.org/10.15252/embj.201797150> PMID: 29930102
27. Sun H, Zhang J, Xin S, Jiang M, Zhang J, Li Z, et al. Cui4-Ddb1 ubiquitin ligases facilitate DNA replication-coupled sister chromatid cohesion through regulation of cohesin acetyltransferase Escoc2. *PLoS Genet*. 2019; 15.
28. Faramarz A, Balk JA, van Schie JJM, Oostra AB, Ghandour CA, Rooimans MA, et al. Non-redundant roles in sister chromatid cohesion of the DNA helicase DDX11 and the SMC3 acetyl transferases ESCO1 and ESCO2. *PLoS One*. 2020; 15.
29. Mayer ML, Gygi SP, Aebersold R, Hieter P. An Alternative RFC Complex Required for Sister Chromatid Cohesion in *S. cerevisiae*. *Mol Cell*. 2001; 7: 959–970. [https://doi.org/10.1016/s1097-2765\(01\)00254-4](https://doi.org/10.1016/s1097-2765(01)00254-4) PMID: 11389843
30. Mayer ML, Pot I, Chang M, Xu H, Aneliunas V, Kwok T, et al. Identification of Protein Complexes Required for Efficient Sister Chromatid Cohesion. *Mol Biol Cell*. 2004; 15: 3751–3737. <https://doi.org/10.1091/mbc.e03-12-0900> PMID: 15181149
31. Skibbens R V. Chl1p, a DNA Helicase-Like Protein in Budding Yeast, Functions in Sister-Chromatid Cohesion. *Genetics*. 2004; 166: 33–42. <https://doi.org/10.1534/genetics.166.1.33> PMID: 15020404
32. Maradeo ME, Skibbens R V. The Elg1-RFC Clamp-Loading Complex Performs a Role in Sister Chromatid Cohesion. *PLoS One*. 2009; 4. <https://doi.org/10.1371/journal.pone.0004707> PMID: 19262753
33. Parnas O, Zipin-Roitman A, Mazor Y, Liefshitz B, Ben-Aroya S, Kupiec M. The Elg1 clamp loader plays a role in sister chromatid cohesion. *PLoS One*. 2009; 4. <https://doi.org/10.1371/journal.pone.0005497> PMID: 19430531
34. Maradeo ME, Skibbens R V. Replication factor C complexes play unique pro- and anti-establishment roles in sister chromatid cohesion. *PLoS One*. 2010; 5. <https://doi.org/10.1371/journal.pone.0015381> PMID: 21060875
35. Maradeo ME, Garg A, Skibbens R V. Rfc5p regulates alternate RFC complex functions in sister chromatid pairing reactions in budding yeast. *Cell Cycle*. 2010; 9: 4370–4378. <https://doi.org/10.4161/cc.9.21.13634> PMID: 20980821
36. Rudra S, Skibbens R V. Sister chromatid cohesion establishment occurs in concert with lagging strand synthesis. *Cell Cycle*. 2012; 11: 2114–2121. <https://doi.org/10.4161/cc.20547> PMID: 22592531
37. Banerji R, Skibbens R V., Iovine MK. Cohesin mediates Escoc2-dependent transcriptional regulation in a zebrafish regenerating fin model of Roberts Syndrome. *Biol Open*. 2017; 6: 1802–1813. <https://doi.org/10.1242/bio.026013> PMID: 29084713
38. Gassler J, Brandão HB, Imakaev M, Flyamer IM, Ladstätter S, Bickmore WA, et al. A mechanism of cohesin-dependent loop extrusion organizes zygotic genome architecture. *EMBO J*. 2017; 36: 3600–3618. <https://doi.org/10.15252/embj.201798083> PMID: 29217590
39. Haarhuis JHI, van der Weide RH, Blomen VA, Yanez-Cuna JO, Amendola M, van Ruiten MS, et al. The Cohesin Release Factor WAPL Restricts Chromatin Loop Extension. *Cell*. 2017; 169: 693–707. <https://doi.org/10.1016/j.cell.2017.04.013> PMID: 28475897
40. Schwarzer W, Abdennur N, Goloborodko A, Pekowska A, Fudenberg G, Loe-mie Y, et al. Two independent modes of chromatin organization revealed by cohesin removal. *Nature*. 2017; 551: 51–56. <https://doi.org/10.1038/nature24281> PMID: 29094699
41. Dauban L, Montagne R, Thierry A, Lazar-Stefanita L, Bastié N, Gadal O, et al. Regulation of Cohesin-Mediated Chromosome Folding by Eco1 and Other Partners. *Mol Cell*. 2020; 77: 1279–1293. <https://doi.org/10.1016/j.molcel.2020.01.019> PMID: 32032532
42. Sumara I, Vorlaufer E, Gieffers C, Peters BH, Peters JM. Characterization of vertebrate cohesin complexes and their regulation in prophase. *J Cell Biol*. 2000; 151: 749–761. <https://doi.org/10.1083/jcb.151.4.749> PMID: 11076961
43. Lavoie BD, Hogan E, Koshland D. In vivo dissection of the chromosome condensation machinery: Reversibility of condensation distinguishes contributions of condensin and cohesin. *J Cell Biol*. 2002; 156: 805–815. <https://doi.org/10.1083/jcb.200109056> PMID: 11864994
44. Woodman J, Hoffman M, Dzieciatkowska M, Hansen KC, Bloom KS. Phosphorylation of the Scc2 cohesin deposition complex subunit regulates chromosome condensation through cohesin integrity. 2015. <https://doi.org/10.1091/mbc.E15-03-0165> PMID: 26354421
45. Shen D, Skibbens R V. Chl1 DNA helicase and Scc2 function in chromosome condensation through cohesin deposition. *PLoS One*. 2017; 12. <https://doi.org/10.1371/journal.pone.0188739> PMID: 29186203

46. Wutz G, Várnai C, Nagasaka K, Cisneros DA, Stocsits RR, Tang W, et al. Topologically associating domains and chromatin loops depend on cohesin and are regulated by CTCF, WAPL, and PDS 5 proteins. *EMBO J.* 2017; 36: 3573–3599. <https://doi.org/10.15252/embj.201798004> PMID: 29217591
47. Rao S, Huang SC, Glenn St Hilaire B, Engreitz JM, Perez EM, Kieffer-Kwon KR, et al. Cohesin Loss Eliminates All Loop Domains. *Cell.* 2017; 171: 305–320. <https://doi.org/10.1016/j.cell.2017.09.026> PMID: 28985562
48. Banerji R, Eble DM, Iovine MK, Skibbens R V. Esco2 Regulates cx43 Expression During Skeletal Regeneration in the Zebrafish Fin. *Dev Dyn.* 2016; 245: 7–21. <https://doi.org/10.1002/dvdy.24354> PMID: 26434741
49. Marston AL. Chromosome Segregation in Budding Yeast: Sister Chromatid Cohesion and Related Mechanisms. *Genetics.* 2014; 196: 31–63. <https://doi.org/10.1534/genetics.112.145144> PMID: 24395824
50. Litwin I, Pilarczyk E, Wysocki R. The Emerging Role of Cohesin in the DNA Damage Response. *Genes (Basel).* 2018; 9. <https://doi.org/10.3390/genes9120581> PMID: 30487431
51. Nishiyama T. Cohesion and cohesin-dependent chromatin organization. *Curr Opin Cell Biol.* 2019; 58: 8–14. <https://doi.org/10.1016/j.ccb.2018.11.006> PMID: 30544080
52. Remeseiro S, Cuadrado A, Carretero M, Martinez P, Drosopoulos WC, Canamero M, et al. Cohesin-SA1 deficiency drives aneuploidy and tumorigenesis in mice due to impaired replication of telomeres. *EMBO J.* 2012; 31: 2076–2089. <https://doi.org/10.1038/emboj.2012.11> PMID: 22415365
53. Lossaint G, Larroque M, Ribeyre C, Bec N, Larroque C, Decaillet C, et al. FANCD2 Binds MCM Proteins and Controls Replisome Function upon Activation of S Phase Checkpoint Signaling. *Mol Cell.* 2013; 51: 678–690. <https://doi.org/10.1016/j.molcel.2013.07.023> PMID: 23993743
54. Lu S, Lee KK, Harris B, Xiong B, Bose T, Saraf A, et al. The cohesin acetyltransferase Eco1 coordinates rDNA replication and transcription. *EMBO Rep.* 2014; 15: 609–617. <https://doi.org/10.1002/embr.201337974> PMID: 24631914
55. Watrin E, Peters J. Cohesin and DNA damage repair. *Exp Cell Res.* 2006; 312: 2687–2693. <https://doi.org/10.1016/j.yexcr.2006.06.024> PMID: 16876157
56. Dorsett D, Strom L. The ancient and evolving roles of cohesin in DNA repair and gene expression. *Curr Biol.* 2012; 22: R240–250. <https://doi.org/10.1016/j.cub.2012.02.046> PMID: 22497943
57. Benedict B, van Schie JJM, Oostra AB, Balk JA, Wolthuis RMF, te Riele H, et al. WAPL-Dependent Repair of Damaged DNA Replication Forks Underlies Oncogene-Induced Loss of Sister Chromatid Cohesion Article WAPL-Dependent Repair of Damaged DNA Replication Forks Underlies Oncogene-Induced Loss of Sister Chromatid Cohesion. *Dev Cell.* 2020; 52: 683–698. <https://doi.org/10.1016/j.devcel.2020.01.024> PMID: 32084359
58. Tong K, Skibbens R V. Pds5 regulators segregate cohesion and condensation pathways in *Saccharomyces cerevisiae*. *Proc Natl Acad Sci.* 2015; 112: 7021–7026. <https://doi.org/10.1073/pnas.1501369112> PMID: 25986377
59. Ben-Aroya S, Koren A, Liefshitz B, Steinlauf R, Kupiec M. ELG1, a yeast gene required for genome stability, forms a complex related to replication factor C. *Proc Natl Acad Sci U S A.* 2003; 100: 9906–9911. <https://doi.org/10.1073/pnas.1633757100> PMID: 12909721
60. Bellaoui M, Chang M, Ou J, Xu H, Boone C, Brown GW. Elg1 forms an alternative RFC complex important for DNA replication and genome integrity. *EMBO J.* 2003; 22: 4304–4313. <https://doi.org/10.1093/emboj/cdg406> PMID: 12912927
61. Kubota T, Nishimura K, Kanemaki MT, Donaldson AD. The Elg1 Replication Factor C-like Complex Functions in PCNA Unloading during DNA Replication. *Mol Cell.* 2013; 50: 273–280. <https://doi.org/10.1016/j.molcel.2013.02.012> PMID: 23499004
62. Kubota T, Katou Y, Shirahige K, Donaldson AD. Replication-Coupled PCNA Unloading by the Elg1 Complex Occurs Genome-wide and Requires Okazaki Fragment Ligation. *Cell Rep.* 2015; 12: 774–787. <https://doi.org/10.1016/j.celrep.2015.06.066> PMID: 26212319
63. Johnson C, Gali VK, Takahashi TS, Kubota T. PCNA Retention on DNA into G2/M Phase Causes Genome Instability in Cells Lacking Elg1. *Cell Reports.* 2016; 16: 684–695. <https://doi.org/10.1016/j.celrep.2016.06.030> PMID: 27373149
64. Longtine MS, McKenzie III A, Demarini DJ, Shah NG, Wach A, Brachat A, et al. Additional Modules for Versatile and Economical PCR-based Gene Deletion and Modification in *Saccharomyces cerevisiae*. *Yeast.* 1998; 14: 953–961. [https://doi.org/10.1002/\(SICI\)1097-0061\(199807\)14:10<953::AID-YEA293>3.0.CO;2-U](https://doi.org/10.1002/(SICI)1097-0061(199807)14:10<953::AID-YEA293>3.0.CO;2-U) PMID: 9717241
65. Tong K, Skibbens R V. Cohesin without cohesion: A novel role for Pds5 in *Saccharomyces cerevisiae*. *PLoS One.* 2014; 9: 1–14. <https://doi.org/10.1371/journal.pone.0100470> PMID: 24963665

66. Lopez-Serra L, Kelly G, Patel H, Stewart A, Uhlmann F. The Scc2–Scc4 complex acts in sister chromatid cohesion and transcriptional regulation by maintaining nucleosome-free regions. *Nat Genet.* 2014; 46: 1147–1151. <https://doi.org/10.1038/ng.3080> PMID: 25173104
67. Baetz KK, Krogan NJ, Emili A, Greenblatt J, Hieter P. The ctf13-30 / CTF13 Genomic Haploinsufficiency Modifier Screen Identifies the Yeast Chromatin Remodeling Complex RSC, Which Is Required for the Establishment of Sister Chromatid Cohesion. *Molecular.* 2004; 24: 1232–1244. <https://doi.org/10.1128/MCB.24.3.1232>
68. Huang J, Hsu JM, Laurent BC. The RSC nucleosome-remodeling complex is required for cohesin's association with chromosome arms. *Mol Cell.* 2004; 13: 739–750. [https://doi.org/10.1016/s1097-2765\(04\)00103-0](https://doi.org/10.1016/s1097-2765(04)00103-0) PMID: 15023343
69. Rowland BD, Roig MB, Nishino T, Kurze A, Uluocak P, Mishra A, et al. Building Sister Chromatid Cohesion: Smc3 Acetylation Counteracts an Antiestablishment Activity. *Mol Cell.* 2009; 33: 763–774. <https://doi.org/10.1016/j.molcel.2009.02.028> PMID: 19328069
70. Sutani T, Kawaguchi T, Kanno R, Itoh T, Shirahige K. Budding Yeast Wpl1(Rad61)-Pds5 Complex Counteracts Sister Chromatid Cohesion-Establishing Reaction. *Curr Biol.* 2009; 19: 492–497. <https://doi.org/10.1016/j.cub.2009.01.062> PMID: 19268589
71. Losada A, Hirano M, Hirano T. Identification of Xenopus SMC protein complexes required for sister chromatid cohesion. *Genes Dev.* 1998; 12: 1986–1997. <https://doi.org/10.1101/gad.12.13.1986> PMID: 9649503
72. Banerjee S, Myung K. Increased Genome Instability and Telomere Length in the *elg1* -Deficient *Saccharomyces cerevisiae* Mutant Are Regulated by S-Phase Checkpoints. *Eukaryot Cell.* 2004; 3: 1557–1566. <https://doi.org/10.1128/EC.3.6.1557-1566.2004> PMID: 15590829
73. Kanellis P, Agyei R, Durocher D. Elg1 Forms an Alternative PCNA-Interacting RFC Complex Required to Maintain Genome Stability. *Curr Biol.* 2003; 13: 1583–1595. [https://doi.org/10.1016/s0960-9822\(03\)00578-5](https://doi.org/10.1016/s0960-9822(03)00578-5) PMID: 13678589
74. Smolikov S, Mazor Y, Krauskopf A. ELG1, a regulator of genome stability, has a role in telomere length regulation and in silencing. *Proc Natl Acad Sci.* 2004; 101: 1656–1661. <https://doi.org/10.1073/pnas.0307796100> PMID: 14745004
75. Davidson MB, Katou Y, Keszthelyi A, Sing TL, Xia T, Ou J, et al. Endogenous DNA replication stress results in expansion of dNTP pools and a mutator phenotype. *EMBO J.* 2012; 31: 895–907. <https://doi.org/10.1038/emboj.2011.485> PMID: 22234187
76. Koc A, Wheeler LJ, Mathews CK, Merrill GF. Hydroxyurea Arrests DNA Replication by a Mechanism That Preserves Basal dNTP Pools. *J Biol Chem.* 2004; 279: 223–230. <https://doi.org/10.1074/jbc.M303952200> PMID: 14573610
77. Tittel-Elmer M, Lengronne A, Davidson MB, Bacal J, Francois P, Hohl M, et al. Cohesin association to replication sites depends on Rad50 and promotes fork restart. *Mol Cell.* 2012; 48: 98–108. <https://doi.org/10.1016/j.molcel.2012.07.004> PMID: 22885006
78. Delamarre A, Barthe A, de la Roche Saint-André C, Luciano P, Forey R, Padioleau I, et al. MRX Increases Chromatin Accessibility at Stalled Replication Forks to Promote Nascent DNA Resection and Cohesin Loading. *Mol Cell.* 2020; 77: 395–410. <https://doi.org/10.1016/j.molcel.2019.10.029> PMID: 31759824
79. Fumasoni M, Zwicky K, Lopes M, Branzei D. Error-Free DNA Damage Tolerance and Sister Chromatid Proximity during DNA Replication Rely on the Pola/Primase/Ctf4 Complex. *Mol Cell.* 2015; 57: 812–823. <https://doi.org/10.1016/j.molcel.2014.12.038> PMID: 25661486
80. Frattini C, Villa-Hernandez S, Pellicano G, Jossen R, Katou Y, Shirahige K, et al. Cohesin Ubiquitylation and Mobilization Facilitate Stalled Replication Fork Dynamics. *Mol Cell.* 2017; 68: 758–772. <https://doi.org/10.1016/j.molcel.2017.10.012> PMID: 29129641
81. Weinert TA, Kiset GL, Hartwell LH. Mitotic checkpoint eenes in budding yeast and the dependence of mitosis on DNA replication and repair. *Genes Dev.* 1994; 8: 652–665. <https://doi.org/10.1101/gad.8.6.652> PMID: 7926756
82. Morrow DM, Tagle DA, Shiloh Y, Collins FS, Hieter P. TEL1, an *S. cerevisiae* Homolog of the Human Gene Mutated in Ataxia Telangiectasia, Is Functionally Related to the Yeast Checkpoint Gene MEC1. *Cell.* 1995; 82: 831–840. [https://doi.org/10.1016/0092-8674\(95\)90480-8](https://doi.org/10.1016/0092-8674(95)90480-8) PMID: 7545545
83. Gobbi E, Cesena D, Galbiati A, Lockhart A, Longhese MP. Interplays between ATM/Tel1 and ATR/Mec1 in sensing and signaling DNA double-strand breaks. *DNA Repair (Amst).* 2013; 12: 791–799. <https://doi.org/10.1016/j.dnarep.2013.07.009> PMID: 23953933
84. Williams RM, Yates LA, Zhang X. Structures and regulations of ATM and ATR, master kinases in genome integrity. *Curr Opin Struct Biol.* 2020; 61: 98–105. <https://doi.org/10.1016/j.sbi.2019.12.010> PMID: 31924595

85. Sun Z, Fay DS, Marini F, Foiani M, Stern DF. Spk1/Rad53 is regulated by Mec1-dependent protein phosphorylation in DNA replication and damage checkpoint pathways. *Genes Dev.* 1996; 10: 395–406. <https://doi.org/10.1101/gad.10.4.395> PMID: 8600024
86. Terret M-E, Sherwood R, Rahman S, Qin J, Jallepalli P V. Cohesin acetylation speeds the replication fork. *Nature.* 2009; 462: 231–234. <https://doi.org/10.1038/nature08550> PMID: 19907496
87. Guillou E, Ibarra A, Coulon V, Casado-Vela J, Rico D, Casal I, et al. Cohesin organizes chromatin loops at DNA replication factories. *Genes Dev.* 2010; 24: 2812–2822. <https://doi.org/10.1101/gad.608210> PMID: 21159821
88. Morales C, Ruiz-Torres M, Rodríguez-Acebes S, Lafarga V, Rodríguez-Corsino M, Megias D, et al. PDS5 Proteins Are Required for Proper Cohesin Dynamics and Participate in Replication Fork Protection. *J Biol Chem.* 2020; 295: 146–157. <https://doi.org/10.1074/jbc.RA119.011099> PMID: 31757807
89. Carvajal-Maldonado D, Byrum AK, Jackson J, Wessel S, Lemacon D, Guitton-Sert L, et al. Perturbing cohesin dynamics drives MRE11 nuclease-dependent replication fork slowing. *Nucleic Acids Res.* 2019; 47: 1294–1310. <https://doi.org/10.1093/nar/gky519> PMID: 29917110
90. Lopez-Serra L, Lengronne A, Borges V, Kelly G, Uhlmann F. Budding yeast Wapl controls sister chromatid cohesion maintenance and chromosome condensation. *Curr Biol.* 2013; 23: 64–69. <https://doi.org/10.1016/j.cub.2012.11.030> PMID: 23219725
91. Guacci V, Koshland D. Cohesin-independent segregation of sister chromatids in budding yeast. *Mol Biol Cell.* 2012; 23: 729–739. <https://doi.org/10.1091/mbc.E11-08-0696> PMID: 22190734
92. Stead K, Aguilar C, Hartman T, Drexel M, Meluh P, Guacci VA. Pds5p regulates the maintenance of sister chromatid cohesion and is sumoylated to promote the dissolution of cohesin. *J Cell Biol.* 2003; 163: 729–741. <https://doi.org/10.1083/jcb.200305080> PMID: 14623866
93. Sikdar N, Banerjee S, Lee K, Wincovitch S, Pak E, Nakanishi K, et al. DNA damage responses by human ELG1 in S phase are important to maintain genomic integrity. *Cell Cycle.* 2009; 8: 3199–3207. <https://doi.org/10.4161/cc.8.19.9752> PMID: 19755857
94. Kenna MA, Skibbens R V. Mechanical link between cohesion establishment and DNA replication: Ctf7p/Eco1p, a cohesion establishment factor, associates with three different replication factor C complexes. *Mol Cell Biol.* 2003; 23: 2999–3007. <https://doi.org/10.1128/mcb.23.8.2999-3007.2003> PMID: 12665596
95. Petronczki M, Chwalla B, Siomos MF, Yokobayashi S, Helmhart W, Deutschbauer AM, et al. Sister-chromatid cohesion mediated by the alternative RF-CCtf18/Dcc1/Ctf8, the helicase Chl1 and the polymerase-associated protein Ctf4 is essential for chromatid disjunction during meiosis II. *J Cell Sci.* 2004; 117: 3547–3559. <https://doi.org/10.1242/jcs.01231> PMID: 15226378
96. Suter B, Tong A, Chang M, Yu L, Brown GW, Boone C, et al. The Origin Recognition Complex Links Replication, Sister Chromatid Cohesion and Transcriptional Silencing in *Saccharomyces cerevisiae*. *Genetics.* 2004; 167: 579–591. <https://doi.org/10.1534/genetics.103.024851> PMID: 15238513
97. Bylund O, Burgers PMJ. Replication Protein A-Directed Unloading of PCNA by the Ctf18 Cohesion Establishment Complex. *Mol Cell Biol.* 2005; 25: 5445–5455. <https://doi.org/10.1128/MCB.25.13.5445>
98. Borges V, Lehane C, Lopez-Serra L, Flynn H, Skehel M, Rolef Ben-Shahar T, et al. Hos1 Deacetylates Smc3 to Close the Cohesin Acetylation Cycle. *Mol Cell.* 2010; 39: 677–688. <https://doi.org/10.1016/j.molcel.2010.08.009> PMID: 20832720
99. McAlear MA, Tuff KM, Holm C. The Large Subunit of Replication Factor C (Rfc1p/Cdc44p) Is Required for DNA Replication and DNA Repair in *Saccharomyces cerevisiae*. *Genetics.* 1996; 142: 65–78. PMID: 8770585
100. Bylund GO, Burgers PMJ. Replication Protein A-Directed Unloading of PCNA by the Ctf18 Cohesion Establishment Complex. *Mol Cell Biol.* 2005; 25: 5445–5455. <https://doi.org/10.1128/MCB.25.13.5445-5455.2005> PMID: 15964801
101. Kang M, Ryu E, Lee S, Park J, Ha NY, Ra JS, et al. Regulation of PCNA cycling on replicating DNA by RFC and RFC-like complexes. *Nat Commun.* 2019; 10. <https://doi.org/10.1038/s41467-019-10376-w> PMID: 31160570
102. Zhang J, Shi X, Li Y, Kim BJ, Jia J, Huang Z, et al. Acetylation of Smc3 by Eco1 Is Required for S Phase Sister Chromatid Cohesion in Both Human and Yeast. *Mol Cell.* 2008; 31: 143–151. <https://doi.org/10.1016/j.molcel.2008.06.006> PMID: 18614053
103. Myung K, Smith S. The RAD5-dependent Postreplication Repair Pathway is Important to Suppress Gross Chromosomal Rearrangements. *J Natl Cancer Inst Monogr.* 2008; 39: 12–15. <https://doi.org/10.1093/jncimonographs/IGN019.The>
104. Li Q, Burgess R, Zhang Z. All roads lead to chromatin: Multiple pathways for histone deposition. *Biochim Biophys Acta.* 2012; 1819: 238–246. <https://doi.org/10.1016/j.bbagr.2011.06.013> PMID: 21763476

105. Ulrich HD. New Insights into Replication Clamp Unloading. *J Mol Biol.* 2013; 425: 4727–4732. <https://doi.org/10.1016/j.jmb.2013.05.003> PMID: 23688817
106. Inoue A, Li T, Roby SK, Valentine MB, Inoue M, Boyd K, et al. Loss of ChIR1 Helicase in Mouse Causes Lethality Due to the Accumulation of Aneuploid Cells Generated by Cohesion Defects and Placental Malformation. *Cell Cycle.* 2007;4101. <https://doi.org/10.4161/cc.6.13.4411> PMID: 17611414
107. Laha S, Das SP, Hajra S, Sanyal K, Sinha P. Functional characterization of the *Saccharomyces cerevisiae* protein Chl1 reveals the role of sister chromatid cohesion in the maintenance of spindle length during S-phase arrest. *BMC Genet.* 2011;12. <https://doi.org/10.1186/1471-2156-12-12> PMID: 21255436
108. Minchell NE, Keszthelyi A, Baxter J. Cohesin Causes Replicative DNA Damage by Trapping DNA Topological Stress Article Cohesin Causes Replicative DNA Damage by Trapping DNA Topological Stress. *Mol Cell.* 2020; 78: 1–13. <https://doi.org/10.1016/j.molcel.2020.03.020> PMID: 32243827
109. Paul Solomon Devakumar LJ, Gaubitz C, Lundblad V, Kelch BA, Kubota T. Effective mismatch repair depends on timely control of PCNA retention on DNA by the Elg1 complex. *Nucleic Acids Res.* 2019; 47: 6826–6841. <https://doi.org/10.1093/nar/gkz441> PMID: 31114918
110. Strom L, Lindroos HB, Shirahige K, Sjogren C. Postreplicative Recruitment of Cohesin to Double-Strand Breaks Is Required for DNA Repair. *Mol Cell.* 2004; 16: 1003–1015. <https://doi.org/10.1016/j.molcel.2004.11.026> PMID: 15610742
111. Sjögren C, Ström L. S-phase and DNA damage activated establishment of Sister chromatid cohesion—importance for DNA repair. *Exp Cell Res.* 2010; 316: 1445–1453. <https://doi.org/10.1016/j.yexcr.2009.12.018> PMID: 20043905
112. New L, Liu K, Crouse G. The Yeast Gene MSH3 Defines a New Class of Eukaryotic MutS Homologues. *Mol Gen Genet.* 1993; 239: 97–108. <https://doi.org/10.1007/BF00281607> PMID: 8510668
113. Putnam CD, Kolodner RD. Pathways and Mechanisms that Prevent Genome. *Genetics.* 2017; 206: 1187–1225. <https://doi.org/10.1534/genetics.112.145805> PMID: 28684602
114. Chakraborty U, Dinh TA, Alani E. Genomic Instability Promoted by Overexpression of Mismatch Repair Factors in Yeast: A Model for Understanding Cancer Progression. *Genetics.* 2018; 209: 439–456. <https://doi.org/10.1534/genetics.118.300923> PMID: 29654124
115. Uhlmann F, Nasmyth K. Cohesion between sister chromatids must be established during DNA replication. *Curr Biol.* 1998; 8: 1095–1102. [https://doi.org/10.1016/s0960-9822\(98\)70463-4](https://doi.org/10.1016/s0960-9822(98)70463-4) PMID: 9778527
116. Intyre JM, Muller EGD, Weitzer S, Snyderman BE, Davis TN, Uhlmann F. In vivo analysis of cohesin architecture using FRET in the budding yeast *Saccharomyces cerevisiae*. *EMBO J.* 2007; 26: 3783–3793. <https://doi.org/10.1038/sj.emboj.7601793> PMID: 17660750
117. Zhang N, Kuznetsov SG, Sharan SK, Li K, Rao PH, Pati D. A handcuff model for the cohesin complex. *J Cell Biol.* 2008; 183: 1019–1031. <https://doi.org/10.1083/jcb.200801157> PMID: 19075111
118. Kulemzina I, Schumacher MR, Verma V, Reiter J, Metzler J, Failla AV, et al. Cohesin Rings Devoid of Scc3 and Pds5 Maintain Their Stable Association with the DNA. *PLoS Genet.* 2012; 8. <https://doi.org/10.1371/journal.pgen.1002856> PMID: 22912589
119. Eng T, Guacci V, Koshland D, Bloom KS. Interallelic complementation provides functional evidence for cohesin–cohesin interactions on DNA. 2015. <https://doi.org/10.1091/mbc.E15-06-0331> PMID: 26378250
120. Cattoglio C, Pustova I, Walther N, Ho JJ, Hantsche-grininger M, Inouye CJ, et al. Determining cellular CTCF and cohesin abundances to constrain 3D genome models. *Elife.* 2019; 8.
121. Lengronne A, Mcintyre J, Katou Y, Kanoh Y, Hopfner K, Shirahige K, et al. Establishment of Sister Chromatid Cohesion at the *S. cerevisiae* Replication Fork. *Mol Cell.* 2006; 23: 787–799. <https://doi.org/10.1016/j.molcel.2006.08.018> PMID: 16962805
122. Song J, Lafont A, Chen J, Wu FM, Shirahige K, Rankin S. Cohesin Acetylation Promotes Sister Chromatid Cohesion Only in Association with the Replication Machinery. *J Biol Chem.* 2012; 287: 34325–34336. <https://doi.org/10.1074/jbc.M112.400192> PMID: 22896698
123. Zheng G, Kanchwala M, Xing C, Yu H. MCM2-7-dependent cohesin loading during S phase promotes sister-chromatid cohesion. *Elife.* 2018; 7. <https://doi.org/10.7554/eLife.33920> PMID: 29611806